

Ultracold Fermi Gases with Emergent $SU(N)$ Symmetry

Miguel A. Cazalilla

*Department of Physics, National Tsing Hua University,
and National Center for Theoretical Sciences, Hsinchu City, Taiwan*

Ana Maria Rey

NIST, JILA and Department of Physics, University of Colorado, Boulder, US

(Dated: February 21, 2024)

We review recent experimental and theoretical progress on ultracold alkaline-earth Fermi gases with emergent $SU(N)$ symmetry. Emphasis is placed on describing the ground-breaking experimental achievements of recent years. The latter include the cooling to below quantum degeneracy of various isotopes of ytterbium and strontium, the demonstration of optical Feshbach resonances and the optical Stern-Gerlach effect, the realization of a Mott insulator of ^{173}Yb atoms, the creation of various kinds of Fermi-Bose mixtures and the observation of many-body physics in optical lattice clocks. On the theory side, we survey the zoo of phases that have been predicted for both gases in a trap and loaded into an optical lattice, focusing on two and three-dimensional systems. We also discuss some of the challenges that lie ahead for the realization of such phases, such as reaching the temperature scale required to observe magnetic and more exotic quantum orders, and dealing with collisional relaxation of excited electronic levels.

Contents

I. Introduction	2
II. Alkaline Earth Fermi gases: An emergent $SU(N)$ symmetry	5
A. Background and Precedents	5
B. Alkaline-earth and Ytterbium Atomic (AEA) Gases	6
C. Relevance of $SU(N)$ symmetry	7
III. Experiments with Trapped Ultracold Gases	9
A. Experimental determination of the scattering length	9
B. Towards a quantum degenerate gas	11
1. Ytterbium	11

	2
2. Calcium	12
3. Strontium	12
C. Control of Interactions: Optical Feshbach resonances	13
D. Imaging and detection of nuclear spin components	14
IV. Experiments in Optical Lattices: Realization of a $SU(6)$ Mott Insulator	15
V. Femi liquids and their instabilities	19
A. $SU(N)$ Fermi liquid theory and Pomeranchuk Instabilities	19
B. BCS Instability and Superfluidity	21
VI. Alkaline-Earth Atoms in Optical lattices	24
A. Cooling on the lattice	24
B. The $SU(N)$ Hubbard model at weak to intermediate coupling	25
C. Strong coupling limit: The $SU(N)$ Heisenberg model	28
VII. Other exotica: Physics beyond the $SU(N)$ Heisenberg model	29
A. Orbital magnetism	29
B. Artificial Gauge fields	30
VIII. Atom-light hybrid systems and many-body physics in optical clocks	31
IX. Summary and Outlook	31
X. Acknowlegments	33
A. Brief Digest of $SU(N)$ Group Theory	33
B. Fermi Liquid Parameters	35
C. Nambu-Goldstone modes of $SU(N)$ superfluids	36
References	37

I. INTRODUCTION

Prior to the late 20th century, matter was primarily something to be probed, dissected, and understood. Now, in the early years of the 21st century, matter is something to be synthesized, organized, and exploited

for broader purposes, both at the level of basic research and for numerous technological applications. One emerging area of research in this century is to ultimately implement Richard Feynman’s pioneering ideas of quantum simulation [1] and quantum information [2]. We want to design in the laboratory artificial, fully controllable quantum systems, and use them to mimic models of many-body systems relevant for otherwise intractable problems in materials physics and other branches of modern quantum Science.

In fact, recent advances in cooling and trapping alkali atoms has brought us closer to realizing Feynman’s dreams. Their simple electronic structure (they possess a single valence electron) has allowed a clean characterization of their hyperfine levels, greatly facilitating the development of extremely effective trapping and quantum control techniques. Using these atoms, major breakthroughs have been achieved such as a detailed understanding of the BEC to BCS crossover [3, 4] and the implementation of both Fermi and Bose Hubbard models [4–8].

Nevertheless, the inherent “simplicity” of alkali atoms introduces major limitations to the phenomena that can be explored with them. For example, the actual observation of quantum magnetism in the Fermi/Bose Hubbard models has been hindered by the low entropy requirements set by the energy scales of the effective spin-spin interactions. In this regard, systems exhibiting more complex internal structure could be an excellent platform for exploring a wider range of many-body phenomena. They also hold the promise of the discovery of new states of matter that go beyond the possibilities already offered by conventional condensed matter systems. During the last few decades, there have been exciting advances in this direction, as new capabilities for cooling, trapping, and manipulating more complex systems such as trapped ions, magnetic atoms, Rydberg atoms, polar molecules, and alkaline-earth atoms have been demonstrated. Here we concentrate our attention on alkaline earth atoms.

Strictly speaking, alkaline-earth atoms (AEA) lie in group-II of the periodic table. However, we will also include others with similar electronic structure like Ytterbium (Yb). These atoms have unique atomic properties which make them ideal for the realization of ultra-precise atomic clocks. Lately, as we shall explain below, they are also attaching a great deal of attention for their interesting many-body physics and the possibilities that they offer for the quantum simulation of complex quantum systems.

Nevertheless, before immersing ourselves in the study of their fascinating many-body physics, it is worth recalling that atomic clocks provide one of the most striking illustrations of the unique advantage of AEA over alkali atoms. State-of-the-art optical atomic clocks use fermionic AEA, such as Sr or Yb [9]. Those clocks have already surpassed the accuracy of the Cs standard [10]. The most stable of these clocks now operate near the quantum noise limit [11, 12] and just recently, thanks to advances in modern precision laser spectroscopy, are becoming the most precise in the world, even surpassing the accuracy of single ion standards [13]. The stability of the neutral atom optical clocks arises from the extremely long lived singlet,

1S_0 , and triplet states 3P_0 , generally referred to as clock states, with intercombination lines both electric and magnetic dipole forbidden and as narrow as a few mHz— nine orders of magnitude lower than a typical dipole-allowed electronic transition (See Fig. 1). It is impossible to achieve this level of clock stability with conventional alkali atoms, due to the decoherence that arises from the intrinsic sensitivity of the hyperfine ground states to magnetic field fluctuations and/or to intensity and phase noise on the optical fields.

Returning to many-body physics and quantum emulation using AEA, in this article we attempt to review the experimental and theoretical progress in this area. Given the large amount of recent research, we mainly focus on the consequences of their emergent $SU(N)$ symmetry of the AEA Fermi gases. Thus, we have tried to capture “snapshots” of the ongoing experimental progress. As far as theory is concerned, we also have attempted to provide a survey of some of the most important and interesting theoretical proposals. Therefore, our selection of topics in the latter regard is rather subjective, and the emphasis has been placed on providing a pedagogical introduction to some of the subjects rather than on providing an exhaustive survey of the available literature. As a consequence, some topics have been left out. For instance, the application of AEA for quantum information purposes will not be discussed here and we refer the interested reader to Ref. [14]. Another topic that we do not touch in depth is the physics of one-dimensional (1D) systems. This subject has been the focus of theoretical interest in recent years, especially concerning quantum magnetism in 1D lattice systems (see e.g. Refs.[15–18] and references therein). For trapped systems on the continuum, we refer the interested reader to the excellent recent review article on this subject by Guan *et al.* [19] and point out that just recently the first experimental exploration of the fascinating role of $SU(N)$ symmetry in an array of 1D fermionic tubes has been reported in Ref. [20].

The outline of this article is as follows: We begin in section II with a review of the work leading to the observation that AEA posses an emergent $SU(N)$ symmetry (for a brief review of the group theory relevant to $SU(N)$, see Appendix A). Although this was a theoretical prediction, it was based on a number of experimental observations associated to the unique atomic structure of AEA. The emergent $SU(N)$ symmetry has not only important consequences in atomic molecular and optical systems and condensed matter physics, many of them reviewed here, but also in other fields in physics as well. In sections III and IV, we review the experiments that have been performed so far both in traps and in optical lattices, respectively. The review of theoretical results begins in section V, where the theory of $SU(N)$ Fermi liquids and their instabilities, including the Bardeen-Cooper-Schrieffer (BCS) instability, are surveyed. Whereas the discussion in this section mainly applies to gases in a trap, in section VI we turn our attention to quantum phases that are intrinsic to lattice systems. Focusing on the deep lattice limit, we discuss both the Fermi Hubbard and Heisenberg models with $SU(N)$ symmetry. Finally, in section VII, we conclude by discussing other interesting models that can be engineered using alkaline-earth atoms. Appendix A contains a brief summary

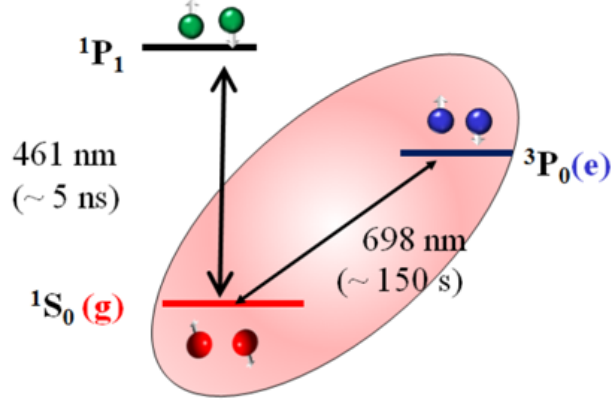


FIG. 1: Energy levels of ^{87}Sr . The singlet, $1S_0$, and the triplet, $3P_0$, states have an inter-combination line as narrow as a few mHz.

of the most important mathematical results about the $\text{SU}(N)$ group and appendices B and C contain some technical details of the topics discussed in section V.

II. ALKALINE EARTH FERMI GASES: AN EMERGENT $\text{SU}(N)$ SYMMETRY

Recently, it has been realized that AEA unique atomic structure has fundamental features which make them attractive for the study of many-body phenomena. One of their most appealing property is an emergent $\text{SU}(N)$ symmetry in the nuclear spin degrees of freedom [21, 22] and many of the consequences arising from it remain to be exploited and understood.

A. Background and Precedents

In order to understand how the $\text{SU}(N)$ symmetry emerges at ultracold temperatures, let us first recall the pioneering work by Lee, Yang, and Huang [23]. These authors considered the thermodynamic description of interacting gases well below their quantum degeneracy temperature and argued that, provided the range of the interactions is much shorter than the inter-particle distance (*i.e.* the gas is “dilute”), the complicated inter-atomic potentials are well approximated by the pseudopotential $V(\mathbf{r}) = \frac{2\pi\hbar^2 a_2}{\mu} \delta(\mathbf{r}) \partial_r [r \cdot]$, where $r = |\mathbf{r}|$ is the relative separation of the colliding particles, μ their reduced mass (= half the bare mass for identical particles), and $a_s = -\lim_{k \rightarrow 0} \delta_s(k)/k$ the scattering length ($\delta_s(k)$ is the s -wave scattering phase-shift). The latter is the only parameter needed to characterize the interactions, since at ultra-low temperatures higher partial waves are suppressed by the centrifugal barrier.

As formulated by Lee, Huang, and Yang, the pseudo-potential applies to bosons and spin- $\frac{1}{2}$ fermions only. It has been later noted by Yip and Ho [24] that for spin- F fermions, this pseudo-potential must be

generalized to:

$$V(\mathbf{r}) = \sum_{\text{even } j=0}^{2F-1} \frac{2\pi\hbar^2 a_s^j}{\mu} \delta(\mathbf{r}) \partial_r [r \cdot] \mathcal{P}_j, \quad (1)$$

where \mathcal{P}_j is the projector onto states with total spin equal to $j = 0, 2, \dots, 2F - 1$. Only the even F values can interact via s -wave collisions since due to quantum statistics those are the only ones that have an associated spatial wavefunction which is anti-symmetric. Hence, it follows that $2F - 1$ scattering lengths are needed to describe the interaction between spin- F fermions. Crudely speaking, the differences between the scattering lengths a_s^0, \dots, a_s^{2F-1} stem from the different configurations the electronic shell of the colliding atoms can adopt for the possible values of F . In the presence of a large magnetic field, F is not longer a good quantum number and the scattering lengths between states with different projection along the quantization direction can become also different [25].

However, Eq. (1) can exhibit a much larger symmetry than naively expected for a higher spin representation of $\text{SU}(2)$. As Wu and coworkers [26] noticed for $F = \frac{3}{2}$, the four-component spinor representation of $\text{SU}(2)$ is isomorphic to a spinor representation of the $\text{SO}(5)$ group without fine tuning. These authors also pointed out that, for the $F = \frac{3}{2}$ members of the AEA family ^{135}Ba and ^{137}Ba , the scattering lengths a_s^2 and a_s^0 should have similar values due to the completely filled outer electronic shell of Barium. These atoms were thus located close to the $\text{SU}(4)$ symmetric line in the phase diagram of Ref. [26].

Alkali gases with approximate $\text{SU}(3)$ symmetries have been considered by a number of authors, beginning with the pioneering work by Modawi and Leggett [27], who studied BCS pairing in a quantum degenerate mixture of the three spin-polarized hyperfine states of ^6Li . Honerkamp and Hofstetter [28, 29] also considered this system as well as mixtures of N hyperfine states of ^{40}K . The three-component ^6Li system has been recently realized experimentally [30, 31] and evidence of the emergence of a $\text{SU}(3)$ symmetry at large magnetic fields (at which the electronic and nuclear spin degrees of freedom start to become decoupled) has been reported. However at moderate magnetic fields the $\text{SU}(3)$ symmetry breaks down.

B. Alkaline-earth and Ytterbium Atomic (AEA) Gases

For the AEA in the ground state (1S_0), the electronic degrees of freedom have neither spin nor orbital angular momentum ($J = 0$). The nuclear spin ($I > 0$), present only in the fermionic isotopes, is thus decoupled from the electronic state due to the absence of hyperfine interactions. Note that all bosonic AEA have $I = 0$ due to their even-even nuclei configuration. Interestingly, the excited state 3P_0 also has, to leading order, vanishing hyperfine interactions and hence highly decoupled nuclear and electronic spins

[32].

The electronic-nuclear spin decoupling in the fermionic isotopes not only allows for an independent manipulation of their nuclear and electronic degrees of freedom, but also imposes the condition that the scattering parameters involving the 1S_0 and 3P_0 states should be independent of the nuclear spin, aside from the restrictions imposed by fermionic antisymmetry. Thus, with great accuracy (see discussion below), in the clock states all the scattering lengths are equal, i.e. $a_s^j = a_s$ (for $j = 0, 2, \dots, 2F - 1$). Under these conditions the interaction and kinetic Hamiltonians become $SU(N)$ spin symmetry (where $N = 2I + 1 = 2F + 1$) [21, 22].

For the 1S_0 it has been theoretically determined that the variation of the scattering length for the various nuclear spin components, should be smaller $\delta a_s/a_s \sim 10^{-9}$ [22]. Although for the 3P_0 electronic state, the decoupling is slightly broken by the admixture with higher-lying P states with $J \neq 0$, this admixture is very small and the resulting nuclear-spin-dependent variation of the scattering lengths is also expected to be very small, of the order of 10^{-3} .

The bounds on the variation of the scattering lengths, $\delta a_s/a_s$ associated to the various nuclear spin projections are based on the fact that the scattering length is just a measure of the semiclassical phase, Φ , accumulated by the colliding atoms from the turning point to infinity (computed at zero energy) [22]. The variation of the phase, proportional to is thus proportional to $\delta a_s/a_s \sim \delta\Phi = \delta V \Delta t / \hbar$, with $\Delta t \sim 1$ ps the total time in the short-range part of the collision and δV the typical energy difference associated with different nuclear spin projections during this time. For the 1S_0 state, the latter can be estimated using second order perturbation theory as $\delta V/h \sim E_{hf}^2/(E_{opt}h) \sim 200$ Hz, where $E_{hf}/h \sim 300$ MHz is the approximate value for the hyperfine splittings in 3P_1 and $E_{opt}/h \sim 400$ THz is the optical energy difference between 1S_0 and 3P_1 . This leads to the 10^{-9} estimate. For the 3P_0 , the second order formula might be incorrect since, the associated molecule states separated by the fine structure energy at large distance may come orders of magnitude closer at short range. Thus to assume $\delta V \sim E_{hf}$ accordingly to first order perturbation theory is a more realistic and conservative estimate, which yields $\delta\Phi \sim 10^{-3}$.

C. Relevance of $SU(N)$ symmetry

It cannot go unnoticed that the availability of fermionic systems exhibiting an enlarged $SU(N)$ symmetry with N as large 10 can be interesting for other fields of physics beyond research on ultracold gases. For instance, in particle physics the theory of quantum chromodynamics (QCD) –which currently provides the most fundamental description of the atomic nucleus and the nuclear interactions– contains two kinds of $SU(3)$ groups. A global flavor $SU(3)$ symmetry group, whose discovery won the Nobel prize for Gell-

Mann, and the gauged color $SU(3)$. The latter describes the origin of the forces that confine the quarks inside baryons and mesons through the exchange of $SU(3)$ gauge bosons known as gluons. In the field of nuclear physics, the $SU(6)$ group has also been considered as candidate to unify the description of baryons and mesons into a single group capable of accounting for both the flavor $SU(3)$ and spin $SU(2)$ symmetries [33]. Indeed, the interesting analogies between ultracold gases with enlarged $SU(N)$ symmetry and cold dense QCD Matter have been already noticed by several authors (see e.g. [21, 34–36] and references therein).

The $SU(N)$ symmetry can also have remarkable consequences in quantum many-body systems. For example in a $SU(2)$ antiferromagnet, which characterize for example spin $1/2$ particles with spin rotation symmetry, every pair of spins minimizes its energy by forming a singlet. The same spin, nevertheless, can participate in only one singlet pair with one of its neighbors. In principle, this constrain can generate geometrical frustration and prevent magnetic ordering. However, spin- $\frac{1}{2}$ particles tend to find a compromise and often become magnetically ordered with decreasing temperature. A typical example of that compromise is found in the $SU(2)$ Heisenberg model on a triangular lattices where, in the ground state, adjacent spins anti-align at 120° degrees.

On the other hand, systems with an enlarged number of degrees of freedom, and exhibiting $SU(N > 2)$ spin rotation symmetry, suffer from massive degeneracies. The latter tend to favor absence of magnetic ordering even classically [37]. Quantum mechanically, this translates into ground states containing massive spin superpositions that give rise to topological order and long range quantum entanglement [38, 39]. Examples of long range quantum entanglement states are fractional quantum Hall states and the ground state of Kitaev's toric code [40].

Indeed, the identification of the $SU(N)$ symmetry as a unique resource for dealing with unconventional magnetic states has a long history in condensed matter physics [41–46]. A generalization of the symmetry from $SU(2)$ to $SU(N)$ introduces a perturbative parameter, namely $1/N$. A large N expansion is particularly useful when dealing with problems of quantum magnetism for which there is no other small parameter that allows for a perturbative treatment. The Kondo impurity problem, the Kondo lattice model [41–43] and the Hubbard model [44–46] are some examples of systems where a large N expansion has been shown to be useful. In such systems, fluctuations about the mean field solutions appear at order $\frac{1}{N}$. The hope is that even at finite N , the $\frac{1}{N}$ corrections can remain irrelevant and thus the mean field solution a good approximation. However, in this context, the enlarged $SU(N)$ symmetry has been often regarded as a mere mathematical construction without a real physical motivation [174] and in many cases just as a means to develop approximate solutions for $SU(2)$ systems. The observation that $SU(N)$ symmetry naturally emerges in the nuclear spin degrees of freedom of fermionic alkaline earth atoms thus raises the exciting potential opportunity of bringing it back to reality and opens the possibility of exploiting its remarkable consequences for the first

time in the laboratory.

Finally, it is also worth mentioning that enlarged unitary symmetries have been also used in other problems in solid state physics, such as the quantum Hall effect in multi-valley semiconductors [47, 48]. In such a systems, the massive degeneracy of the Landau levels is supplemented by a large degeneracy in spin and valley-spin, which favors ferromagnetic states and complex spin-valley textures [47, 48]. A recent revival of the interest in these systems has been brought by graphene [49], which can be regarded as a two-valley zero-gap semiconductor. Graphene exhibits a $SU(4)$ spin-valley symmetry [49, 50], which, although weakly broken by the long-range part of the Coulomb interaction, plays an important role in determining the properties of the ground state both in the integer [51, 52] and fractional quantum Hall effect [50, 53]. Finding connections between these phenomena and the many-body physics of AEA remains an interesting challenge for both experimentalists and theorists.

III. EXPERIMENTS WITH TRAPPED ULTRACOLD GASES

Owing to their unique properties, recently, substantial experimental efforts have been directed at cooling, trapping, and manipulating AEA and many of the capabilities previously demonstrated with alkaline atoms are starting to be reproduced with AEA. These include laser cooling down to microKelvin temperatures, trapping in optical potentials for several seconds, evaporative cooling to quantum degeneracy, the demonstration of a high degree of control over both internal and external degrees of freedom, imaging and resolving the various hyperfine components using optical Stern-Gerlach, demonstrating control of interaction parameters via optical and magnetic Feshbach resonance, and the realization of a Mott Insulator. In this section, we first present a summary of those experimental developments for trapped gases. In the following section, we review the experiments dealing with Fermi gases on optical lattices.

A. Experimental determination of the scattering length

A natural manifestation of the $SU(N)$ symmetry is the conservation of each of the nuclear spin components during a collision. This is in stark contrast to the smaller $SU(2)$ symmetry exhibited by alkali atoms which allows for spin changing processes for $F > \frac{1}{2}$. This is because, as described in section II A, for the latter the scattering lengths depend on the total $F = J + I$ of the colliding atoms and therefore, during collisions the bare nuclear spin degrees of freedom get effectively mixed. Thus, even though the total spin magnetization (m_F) is always conserved, it is possible to have spin changing collisions, for example between two atoms with angular momentum projection $m_F = 0$, into one in $m_F = 1$ and the other in

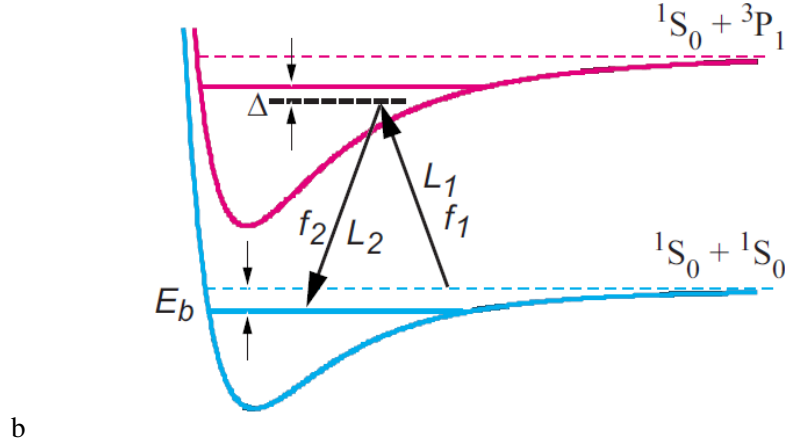


FIG. 2: (Reproduced from Ref. [57]) Schematic description of the two-color PA spectroscopy. The laser L_1 drives the one-color PA transition. The laser L_2 couples the bound state in the excited molecular potential to the one in the ground molecular potential. The detuning of the PA laser with respect to the one-color PA resonance is set to several MHz for the Raman spectroscopy, while is set to zero for the Autler-Townes spectroscopy

$$m_F = -1.$$

As emphasized above, although the s -wave scattering length is the only parameter that fully characterizes the collisional properties of ultra-cold gases, it is very sensitive to the ground state interatomic potential, and thus naive ab initio calculations in general fail to determine it [54]. Consequently, we need to rely on experiments for its actual determination. Among those experiments, we can mention: cross-dimensional rethermalization measurements, time of flight images, and one and two-color photo-association spectroscopy.

Two-color photo-association (TPA) uses two laser beams to measure the binding energy of the weakly bound states of a molecular system [55] (See Fig. 2). One, L_1 , which probes a transition between a pair of colliding ground state atoms and a excited molecular bound state, and a second, L_2 , which probes the bound-bound transition between the excited molecular bound state and a ground molecular bound-state close to the dissociation threshold. If L_2 is close to resonance to the bound-bound transition, it causes the so called Autler-Townes doublet [56] and when the laser L_1 is also on resonance to the free-bound transition, the atomic loss coming from the population of the molecular excited state is suppressed due to quantum interference (Autler-Townes spectroscopy). On the contrary, if both lasers are off-resonant and the frequency difference matches the binding energy of the ground molecular state, the lasers drive a stimulated Raman transition from the colliding atom pair to the molecular ground state which can be detected as an atom loss (Raman spectroscopy).

For AEA two-color photo-association (TPA) has become the most reliable and precise way to determine ground state scattering lengths. This is because the absence of hyperfine structure in the 0S_1 state (with no electronic orbital and spin angular momenta) gives rise to a simple isotope-independent ground state

Atom Species	Mass (u)	Nuclear Spin (I)	Symmetry Group	Scattering Length (nm)
^{171}Yb	170.93	$\frac{1}{2}$	SU(2)	$-0.15(19)$ [^{171}Yb], $-30.6(3.2)$ [^{173}Yb] [57]
^{173}Yb	172.94	$\frac{5}{2}$	SU(6)	$10.55(11)$ [^{173}Yb], $-30.6(3.2)$ [^{171}Yb] [57]
^{87}Sr	86.91	$\frac{9}{2}$	SU(10)	$5.09(10)$ [^{87}Sr] [58]

TABLE I: Table of fermionic alkaline-earth atom (AEA) characteristics. The data is for the AEA species that have been so far cooled down to quantum degeneracy.

molecular potential. The number of bound states in the molecular potential, which can be cleanly extracted from TPA can then be used as an input parameter in a semiclassical theory [54] which, together with mass scaling, can determine the scattering length of all isotopes with unprecedented precision.

In Table I we display the measured values of the s -wave scattering lengths for various fermionic AEA along with other relevant data, such as their mass, nuclear spins and emergent $\text{SU}(N)$ symmetries. Note that the scattering length can vary from large negative to large positive values. The magnitude of the s -wave scattering length determines the feasibility of reaching quantum degeneracy for the various isotopes via evaporative cooling methods.

B. Towards a quantum degenerate gas

1. Ytterbium

The quest of achieving a quantum degenerate gas with group-II atoms started with Yb. Yb has five stable bosonic isotopes $^{168,170,172,174,176}\text{Yb}$ and two fermionic isotopes, ^{171}Yb with $I = 1/2$ and ^{173}Yb with $I = 5/2$.

The first experimental realization of a Bose Einstein Condensate (BEC) of ^{174}Yb was reported in 2003 by the Kyoto group [59]. The lack of hyperfine structure in the ground state of bosonic AEA prevents the use of the conventional magnetic trap for BEC production and evaporative cooling by a radio frequency knife. Instead, all-optical trapping and cooling methods are needed. Four years later, in 2007 all-optical formation of degenerate fermionic ^{173}Yb gas was achieved by the Kyoto group by performing evaporative cooling of the six-nuclear spin-state mixture in the optical dipole trap [60]. Following it, a BEC of ^{170}Yb [61] and ^{176}Yb [62] were reported by the same group. The latter required sympathetic cooling of ^{176}Yb with ^{174}Yb , due to the fact that ^{176}Yb has a negative scattering length. A rapid atom loss in ^{176}Yb atoms seen after cooling down the gas below the transition temperature was consistent with the expected collapse of a ^{176}Yb condensate due to attractive interactions.

The ^{171}Yb fermionic isotope has a very small scattering length in its ground state, $a_s \approx -0.15$ nm,

which prevents cooling by direct evaporation. However, in 2010 it was cooled to quantum degeneracy via sympathetic cooling with ^{176}Yb . This allowed to realize, in the presence of ^{173}Yb , the first $\text{SU}(2) \times \text{SU}(6)$ mixture in ultra-cold gases [63]. Finally, despite the low natural abundance of ^{168}Yb , of the order of 0.13%, a BEC of this rare atomic species was obtained by direct evaporative cooling in 2011 [64]. Thus, except from ^{172}Yb , which is unstable to three body losses due to its large negative scattering length, quantum degenerate gases and/or mixtures of all the stable Yb isotopes have been produced by the Kyoto group. Recently the creation of quantum degenerate gases of Ytterbium has been also reported by Sengstock's group in Hamburg [65]. The production of quantum degenerate mixtures of fermionic alkali-metal ^6Li and bosonic Yb [66, 67] and fermionic Yb [67] has also been reported.

2. Calcium

Calcium was the first AEA, truly belonging to the group-II elements of the periodic table, which was cooled down to quantum degeneracy. In 2009 at PTB (Germany) a BEC of ^{40}Ca was reported [68]. This was achieved in spite of the inelastic collisions associated with its large ground state s -wave scattering length ($18\text{nm} < a_s < 37\text{nm}$) [58], by using a large volume optical trap for initial cooling. A second Calcium BEC was reported in 2012 by Hemmerich's group in Hamburg [69]. So far, no fermionic isotopes of Ca have have been cooled below the quantum degeneracy temperature.

3. Strontium

Strontium has three relatively abundant isotopes. Two of them are bosonic ^{86}Sr and ^{88}Sr with relative abundance $\approx 9.9\%$ and $\approx 82.6\%$ respectively and one fermionic ^{87}Sr with $\approx 7.0\%$ and a nuclear spin $I = 9/2$.

Initial efforts to reach quantum degeneracy with Sr gases failed due the unfavorable scattering properties of the bosonic isotopes [70, 71]. While the scattering length of ^{88}Sr is close to zero, the scattering length of the ^{86}Sr isotope is very large, $a_s \approx 40\text{ nm}$, leading to large detrimental loss of atoms by three-body recombination. The breakthrough for reaching quantum degeneracy came from the development of an efficient loading scheme which allowed to overcome the low natural abundance of ^{84}Sr (only $\approx 0.56\%$) and to take advantage of its favorable scattering length, $a_s \approx 6.5\text{ nm}$. A BEC of ^{84}Sr was almost simultaneously reported by two groups, Schreck's group (Insbruck) [72] and Killian's group (Rice University at Texas) [73]. This achievement was followed up by the cooling to quantum degeneracy of a spin polarized gas ^{87}Sr in thermal contact with a BEC of ^{84}Sr [74] and the corresponding mixture [75] by the same groups respectively.

A BEC of ^{86}Sr was finally created, in spite of its large scattering length, by the Innsbruck group. This was achieved by reducing the density in a large volume optical dipole trap [76, 77]. Furthermore, a BEC of ^{88}Sr was produced by the Rice group, which used sympathetic cooling with ^{87}Sr [78]. Finally, the quest of developing faster and better pure optical methods towards reaching larger and colder samples of AEA has recently lead to the implementation of a method based on laser cooling as the only cooling mechanism [79].

C. Control of Interactions: Optical Feshbach resonances

The ability to tune interactions in ultracold alkali-metal atomic gases using magnetic Feshbach resonances (MFR) has been a crucial step for the exploration of few and many-body physics in these systems [25]. MFR, however, can not be used to tune interactions in ground state of AEA due to the lack of magnetic electronic structure.

However, tuning interatomic interactions via Optical Feshbach resonances (OFR) is a feasible route in AEA. In a OFR a laser tuned near a photoassociative resonance is used to couple a pair of colliding atoms to a bound molecular level in an excited electronic level. The coupling induces a Feshbach resonance and modifies the scattering length of the two colliding atoms. In Ref. [80] it was predicted that OFR could be ideally implemented in AEA using a transition from the singlet ground state to a metastable triplet level. The possibility of tuning the scattering length with significantly less induced losses was based on the long lifetime of the excited molecular state and a relatively large overlap integral between excited molecular and ground collisional wavefunctions.

There has been already a few experimental demonstrations of the use of OFR to modify interaction properties in AEA, although significant atom loss has always been observed. The modification of the photoassociation spectrum by an OFB in a thermal gas of ^{172}Yb was reported in Ref. [81]. An OFR laser pulse of a 1D optical lattice turned on for several microseconds was used in Ref. [82] to modulate the mean field energy in a ^{174}Yb BEC. In Ref. [83] an OFR in a thermal gas of ^{88}Sr was used to modify its thermalization and loss rates. More recently an OFR in Ref. [84] was used to control the collapse and expansion of a ^{88}Sr BEC by moderate modifications of the scattering length. The use of more deeply bound excited molecular states to help the suppression of atom-light scattering and to reduce the background two-body loss could enhance the utility of OFR in AEA and efforts in that direction are currently taking place in various labs. One important point to highlight, nevertheless, is that the direct use of OFR to control scattering properties can destroy the $\text{SU}(N)$ symmetry since the ground state is directly coupled to an excited state which does possess a hyperfine structure.

D. Imaging and detection of nuclear spin components

An important tool for probing AEA is the ability to separately resolve the different nuclear spin components (see Fig. 3). In group-I elements like alkali atoms hyperfine states can be resolved and imaged by taking advantage of the well known Stern-Gerlach technique. The latter uses the spin-state dependent force generated by a magnetic-field gradient to spatially split an expanding atom cloud in clouds of different hyperfine levels. However, this method cannot be used for AEA in the clock states for which $J = 0$, due to their small magnetic moment which entirely stems from the nuclear spin. Let us recall that the nuclear magnetic moment is about three orders of magnitude smaller than the Bohr magneton and therefore the separation of the nuclear components would require inaccessible magnetic field gradients. To overcome this difficulty, experiments have successfully taken advantage of the called Optical Stern-Gerlach (OSG) effect produced by circularly polarized laser beams. The basic idea is that the spin-dependent light shift generated by circularly polarized beams mimics a fictitious magnetic field, which can be used to resolve the nuclear manifold [85]. For the ^{173}Yb gas [63] one OSG beam was sufficient to separate four of the six nuclear spin states. The remaining two nuclear states could be analyzed by reversing the polarization of the OSG beam. For a ^{87}Sr gas, the simultaneous application of two OSG beams with opposite circular polarization was required to resolve all the nuclear spin states [86].

An alternative and complementary tool to resolve nuclear spin components uses spectroscopic methods. These are ideal for AEA thanks to their narrow intercombination lines. The first demonstration of this technique was achieved using the ultra-narrow 1S_0 - 3P_0 transition in an optical lattice clock [32] operated with a cool (at temperature of a few μK) but not quantum degenerate ^{87}Sr gas. The 1S_0 - 3P_0 is only allowed (laser light couples weakly to the clock states) because in the excited state, the hyperfine interaction leads to a small admixture of the higher-lying P states [87]. This small admixture strongly affects the magnetic moment, so that the nuclear g factor of the excited state significantly differs from that of the ground state (i.e. $\sim 50\%$ for strontium). The differential g factor was used to resolve all ten nuclear spins in a bias magnetic field. The spectroscopy was performed in a deep one dimensional optical lattice designed to operate at the so-called magic wavelength, at which the light shifts on the clock states are equal and the clock frequency is not perturbed by them [88]. A similar procedure but using instead the 1S_0 - 3P_1 intercombination line was used in Ref. [86] to perform nuclear spin dependent absorption imaging.

A fundamental consequence of the $\text{SU}(N)$ symmetry is the conservation of the total number of atoms with nuclear spin projection m_I , $-I \leq m_I \leq I$. This means that an atom with large I such as ^{87}Sr can reproduce the dynamics of atoms with lower I if one takes an initial state with no population in the extra levels. Ref. [86] tested this fundamental feature by measuring spin-relaxation using the nuclear-spin-state

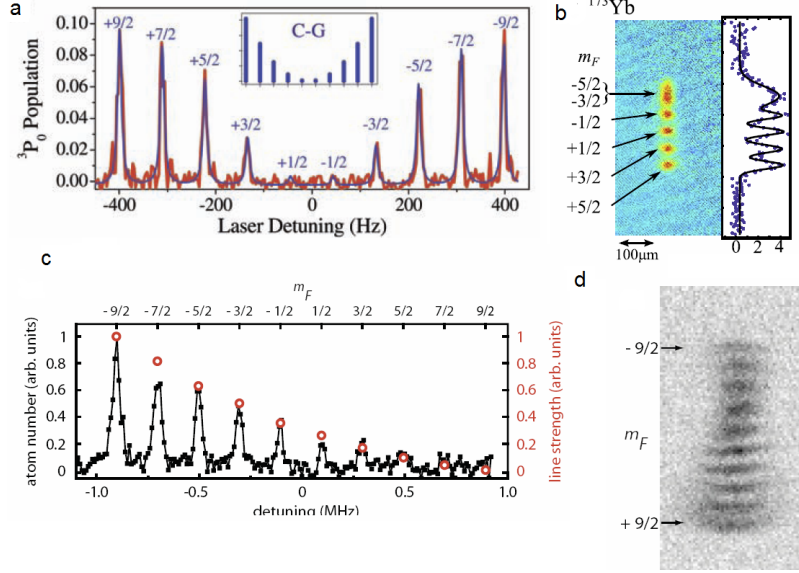


FIG. 3: Experimental resolution of the nuclear spin sublevels: a) Spectroscopically interrogating the 1S_0 - 3P_0 transition in an optical lattice clock [32] operated with ^{87}Sr gas, b) in a quantum degenerate gas of ^{173}Yb using Optical Stern-Gerlach (OSG) [63], c) Spectroscopically using the 1S_0 - 3P_1 intercombination line in a cold quantum gas of ^{87}Sr atoms at a temperature of $0.5\mu\text{K}$ [86] and d) using Optical Stern-Gerlach (OSG) in a quantum degenerate ^{87}Sr gas [86].

detection techniques described above. The spin-relaxation rate constant was found to be less than $5 \times 10^{-15} \text{ cm}^3\text{s}^{-1}$.

IV. EXPERIMENTS IN OPTICAL LATTICES: REALIZATION OF A $\text{SU}(6)$ MOTT INSULATOR

Optical lattices provide us with a new way of studying ultracold atomic gases by confining them in periodic arrays that strongly resemble the potential experienced by electrons in crystalline solids. The optical lattice potential is highly controllable and can be used to tune the interatomic interactions, the density, the kinetic energy and even the dimensionality of the system by tightly confining the atoms along specific directions (see *e.g.* Refs. [4, 89, 90] for a review and references therein).

AEA gases trapped in optical lattices realize the $\text{SU}(N)$ generalization of the Hubbard model [21, 63] [175]:

$$H = -t_g \sum_{\langle i,j \rangle} \left[c_{\alpha i}^\dagger c_j^\alpha + \text{h.c.} \right] + \frac{U_{gg}}{2} \sum_i n_i(n_i - 1), \quad (2)$$

where $\sum_{\langle i,j \rangle}$ stands for summation over nearest-neighbor lattice sites. $c_{\alpha i}$ are fermionic annihilation operators of g atoms in nuclear spin α at lattice site i . The lattice site index i is associated with the vector $\mathbf{R}_i = (R_{x_i}, R_{y_i}, R_{z_i})$, where $R_{r_i} = m_{r_i}a$ ($r = x, y, z$), m_{r_i} being positive integers and a the lattice param-

eter. $n_i = c_{\alpha i}^\dagger c_i^\alpha$ is the operator that measures the total fermion occupation (irrespective of the spin) at the lattice site i . The dimensionality of the lattice, d , and the lattice spacing a are determined by the number of counter-propagating laser beams employed to create the lattice potential and the laser wavelength respectively [4, 89]. Equation (2) describes the dynamics of a dilute ultracold Fermi gas hopping between nearest neighbour lattice sites and interacting only locally. The lattice potential is assumed deep enough that only the lowest Bloch band is occupied by the atoms. In this regime at most N fermions can occupy the same lattice site.

The Hubbard model is written in a form that is manifestly $SU(N)$ invariant. It is characterized by two energy scales, t_g and U_{gg} , which correspond to the kinetic and interaction energy, respectively, and are determined by the depth of the optical lattice potential [4, 63]. U_{gg} is proportional to a_s , i.e. the s -wave scattering length between two atoms in the ground state. Experimentally, the ratio U_{gg}/t_g can be tuned by varying the depth of the lattice potential, which in turn is controlled by the intensity of the laser beams generating the lattice [4].

Roughly speaking, at absolute temperatures $T \ll t_g/k_B$, when the kinetic energy dominates (i.e. $t_g \gg U_{gg}$) and away from special values of the lattice filling, $n = \langle n_i \rangle$, the system is expected to be a Fermi liquid (see section V). On the other hand, when the lattice filling, n , takes integer values $n < N$, and the interaction energy dominates, i.e. $U_{gg} \gg t_g$, the hopping of the atoms between lattice sites is strongly suppressed. This is because, in order to be able to move around, atoms must pay an energy penalty $\approx U_{gg}$, which at low temperatures $T \ll U_{gg}/k_B$ is not available. Thus, the system becomes a Mott insulator, for which atom motion is blocked by interactions. This situation is different from the so called band insulator which happens when $n = N$. In this case the lowest Bloch band is completely filled and the atom motion is blocked, even in the absence of interactions, by the Pauli exclusion principle.

The experiment reported in Ref. [63], describes the realization of the $SU(6)$ Hubbard model by loading an nuclear spin mixture of ^{173}Yb atoms in their ground state ($g = ^1S_0$) in a three-dimensional cubic optical lattice with lattice spacing $a = 266$ nm. The lattice was generated by $d = 3$ mutually orthogonal pairs of counter-propagating laser beams. In addition to the two terms in Eq. (2), in the experiments there is a confining potential generated by the Gaussian curvature of the lattice beams. The latter is described by adding to Eq. (2) the term:

$$V_{\text{trap}} = \sum_i V_i n_i. \quad (3)$$

The trapping potential is well approximated by a harmonic trap, i.e. $V_i = \frac{1}{2} \sum_{r=x,y,z} m \omega_r^2 a^2 / 2 \left(\frac{R_{r_i}}{a} \right)^2$,

where ω_r is the trap frequency along the $r = x, y, z$ directions (for example $\omega \approx 2\pi \times 100$ Hz in Ref. [63]).

In order to realize a Mott insulator with $SU(N = 6)$ symmetry, the Kyoto group followed the standard adiabatic loading procedure used to create Mott insulators in alkali-metal gases [4]. Specifically, an ultracold gas of ^{173}Yb atoms was first loaded in a 3D dipole trap and then into a deep optical lattice by ramping slowly the lattice depth up to a maximum final value of $13 E_R$ ($E_R = \hbar^2 \pi^2 / m a^2$ being the recoil energy of the atoms). The loading was checked to be adiabatic by reversing the ramp of the optical lattice and finding that the initial and final temperatures were very close to each other. For the final trapping conditions quoted above and the initial temperature of the gas ($T_i/T_F \approx 0.2$), the maximum lattice filling was below 2 atoms per site even at the center of the trap. This condition is crucial for probing the Mott insulator phase.

To probe the $SU(6)$ Mott phase and, in particular, to infer its temperature, the Kyoto group used lattice modulation spectroscopy [91–94]. The latter applies a small periodic (in time) modulation to the optical lattice depth, which heats the gas. When the system enters the Mott phase, the injected energy causes the creation of holes and doublons, i.e. empty sites and doubly-occupied sites, respectively. The doublons production rate (DPR) can be measured by converting the doublons into molecules via photo-association. The molecules escape very fast from the trap and thus can be detected as atom loss. For deep lattices, the DPR as a function of frequency exhibits a peaked distribution centered at the frequency corresponding to the Mott gap ($\approx U_{gg}/\hbar$ for $U_{gg} \gg t_g$, see Fig. 4). Hence, the lattice modulation provides a direct measurement of the Mott gap. This technique can be also used to estimate the temperature of the gas in the lattice, which sets the system in the regime $t_g^2/U_{gg} \ll t_g < k_B T < U_{gg}$ [63]. Theoretical calculations based on slave particle methods and high-temperature series expansions [94] agreed with the experimental observations.

By comparing the temperature measurements taken for the Mott insulating phases of $SU(6)$ and $SU(2)$ gases (the latter achieved by optical pumping, remember N can be controlled by initial state preparation) it was found that the final temperature for the $SU(6)$ gas was a factor of ~ 2 or 3 smaller than the one they reached for the $SU(2)$ system (see figure 5). The initial T_i/T_F values, achieved as a result of evaporative cooling, were almost the same for both the $SU(2)$ and $SU(6)$ cases –not the bare temperature–.

These measurements were consistent with the theoretical expectations that systems with $SU(N > 2)$ symmetry, adiabatically loaded on a lattice, can be more efficiently cooled down than $SU(2)$ systems [21, 96]. The cooling can be understood as a direct consequence of the large entropy stored in the spin degrees of freedom in a $SU(N)$ Mott insulator in the $t_g < k_B T < U_{gg}$ regime. See Sec. VI for a more detailed discussion.

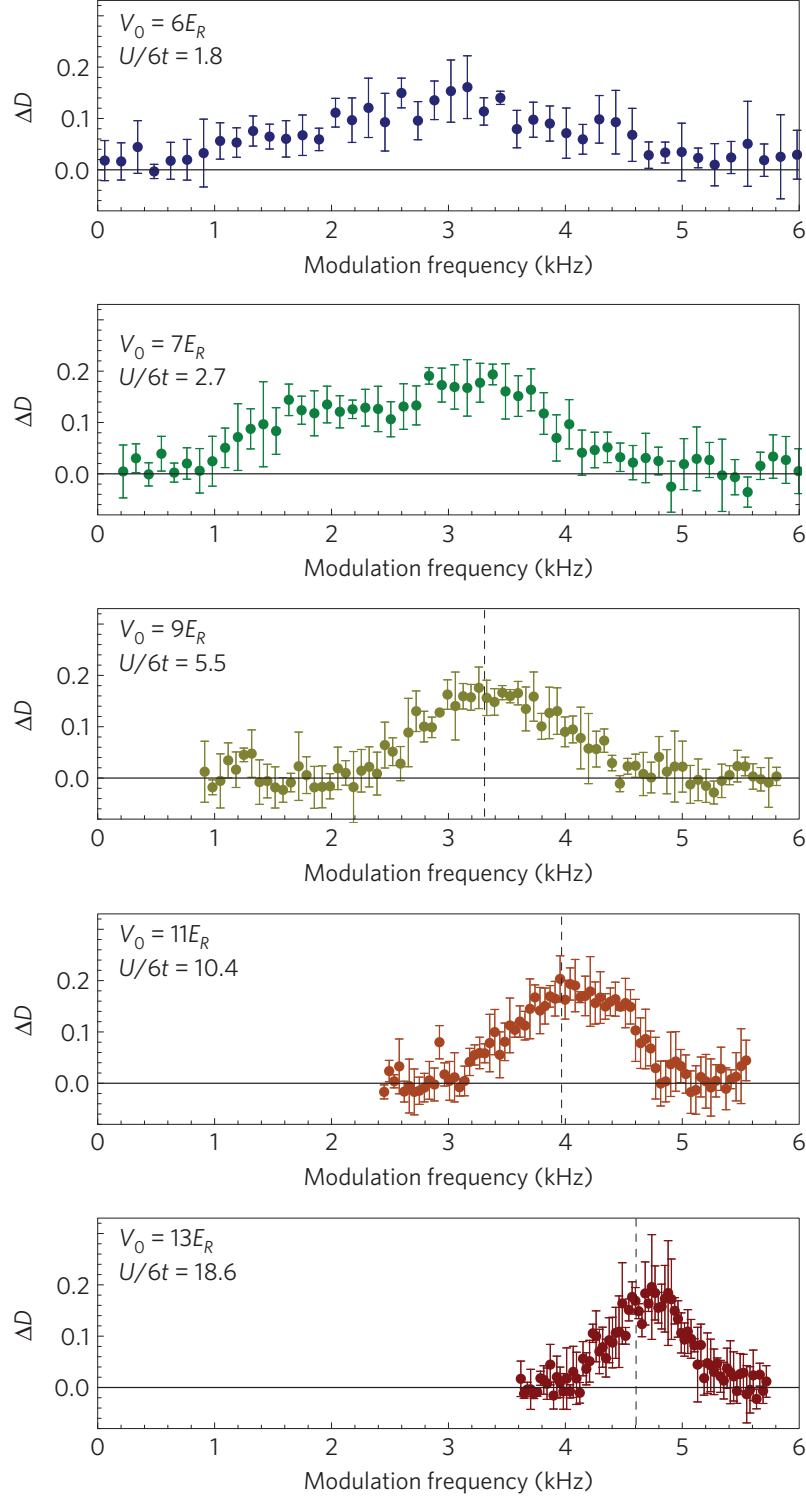


FIG. 4: Lattice modulation spectra vs. modulation frequency for increasing values of the lattice depth (measured in units of the ^{173}Yb recoil energy, E_R). The series shows the emergence of a peak centered around the frequency corresponding to the Mott gap.

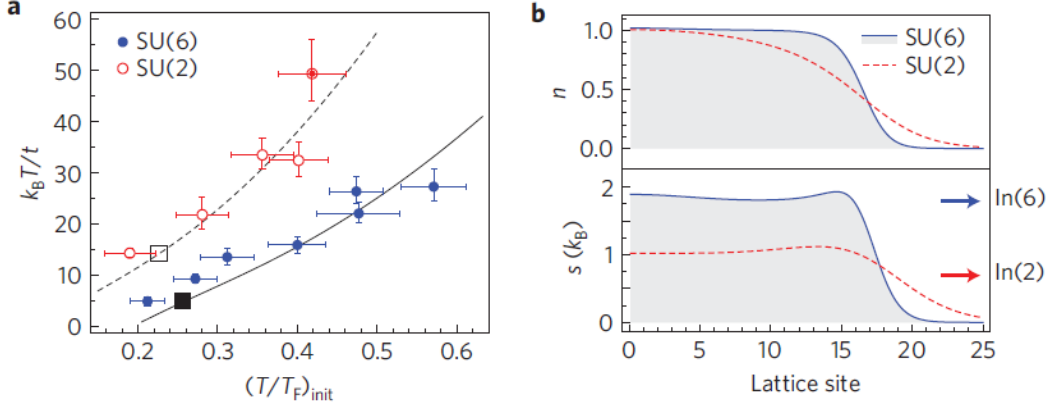


FIG. 5: Adiabatic loading of a $SU(N)$ insulator. From Ref. [95]: a) Temperatures of $SU(6)$ and $SU(2)$ Fermi gases in the lattice inferred from doublon production rate. The atom number is $1.9(1) \times 10^4$, the lattice depth is $11E_R$ ($t/h = J_{gg}/h = 63.7$ Hz and $U/h = U_{gg}/h = 4.0$ kHz). The dependence on the initial temperature in the harmonic trap is shown. The solid and dashed lines are the corresponding theoretical curves that assume adiabatic loading into the lattice [96], and the square boxes indicate the conditions for which the calculations in b) were performed. b) Calculated density (top) and entropy distribution (bottom) at the lowest measured temperatures for the six and two-component cases, indicated by squares in a. The maximum spin entropy $\ln(N = 6, 2)$ is indicated by the arrows.

V. FEMI LIQUIDS AND THEIR INSTABILITIES

A. $SU(N)$ Fermi liquid theory and Pomeranchuk Instabilities

At temperatures well below the Fermi Temperature T_F , in a trap or in an optical lattice of weak to moderate trap depth, a gas of AEA atoms is expected to be a Fermi liquid. The latter defines a universality class of interacting fermion systems. As introduced by Landau [97] (see *e.g.* Ref. [98] for a review), Fermi liquids are characterized by the existence of a gapless Fermi surface (FS) and long-lived low-energy fermionic elementary excitations known as quasi-particles (QP). The QP states can be put in one-to-one correspondence with the excited states of a non-interacting Fermi gas, which implies that QPs carry the same quantum numbers as non-interacting particles in a Fermi gas.

For a uniform $SU(N)$ symmetric AEA Fermi liquid, the above statements mean that momentum and $SU(N)$ (nuclear) spin are good quantum numbers, and therefore a QP distribution function in momentum space, $n_\alpha(\mathbf{p})$, can be defined. At $T = 0$, the ground state of an unpolarized three-dimensional gas of mean density $\rho_0 = N_0/V$ is described by a Fermi distribution QP given by $n_\alpha(\mathbf{p}) = n_0(p) = \theta(p - p_F)$, where $p_F = \left(\frac{4\pi^2\rho_0}{N}\right)^{1/3}$ is the radius of the FS. In order to describe excitations, it is useful to generalize the QP distribution function to a density matrix, $n_\beta^\alpha(\mathbf{p})$, which allows us to describe excited states in which the different orientations of the nuclear spin may be entangled. Following Landau, the grand-canonical free

energy (at $T = 0$) of the excited states can be written as [21, 99]:

$$F = F_0 + \sum_{\mathbf{p}} [\epsilon_0(\mathbf{p}) - \mu] \delta n_{\alpha}^{\alpha}(\mathbf{p}) + \frac{1}{2V} \sum_{\mathbf{p}, \mathbf{p}'} f_{\alpha\gamma}^{\beta\delta}(\mathbf{p}, \mathbf{p}') \delta n_{\beta}^{\alpha}(\mathbf{p}) \delta n_{\delta}^{\gamma}(\mathbf{p}'), \quad (4)$$

where $\epsilon_0(\mathbf{p})$ is the bare quasi-particle energy, μ the zero-temperature chemical potential, and $\delta n_{\beta}^{\alpha}(\mathbf{p}) = n_{\beta}^{\alpha}(\mathbf{p}) - n_0(p) \delta_{\beta}^{\alpha}$ is the deviation of the QP distribution with respect to the ground state. For $p \approx p_F$, $\epsilon_0(\mathbf{p}) = \mu + \frac{p_F}{m^*}(p - p_F)$, where m^* is the QP mass and μ the zero-temperature chemical potential.

In Eq. (4) $f_{\alpha\gamma}^{\beta\delta}(\mathbf{p}, \mathbf{p}')$ is the Landau function that describes the (forward scattering) interactions between the QPs. As explained in the Appendix B, the Landau function can be parametrized in terms of discrete set of Landau parameters $\{F_L^{\rho}, F_L^m\}$, where $L = 0, 1, 2, \dots$ is an integer. The Landau parameters can be obtained, to lowest order in the gas parameter $p_F a_s$ using the Hartree-Fock approximation. This yields $F_0^{\rho} \simeq 2(N-1)p_F a_s/\pi$ and $F_0^m \simeq -2p_F a_s/\pi$, and vanishing values for $L > 0$ (hence, $m^* = m$) [21]. Recently, they have also obtained to second order in $p_F a_s$ [100]. The higher order corrections are much enhanced at large N . This means, in particular, that the region at which the Hartree-Fock (HF) results apply rapidly shrinks with N because the applicability criterion for HF is $N k_F a < 1$.

For the isotropic Fermi liquid state to be stable, the positivity of the free energy fluctuations to quadratic order requires that $F_L^{\rho, m} > -(2L+1)$, otherwise the system undergoes a Pomeranchuk instability [21, 98, 99] that can result in a permanent deformation of the FS, which may or may not be accompanied by a spontaneous breaking of the $SU(N)$ symmetry. A notable example of Pomeranchuk instability is Stoner instability, which corresponds to the transition from an spin unpolarized (i.e. paramagnetic) to a polarized gas. For a system in a trap, where number of particles in each component is fixed, this transition corresponds to the spatial segregation of the different nuclear spin components.

Within Landau Fermi liquid theory, the Stoner instability happens if $F_0^m < -1$. Interestingly, to lowest order in $p_F a_s$, this criterion is $p_F a_s \simeq \frac{\pi}{2}$, which is the same for all N [21]. Yet, the analysis based on Fermi liquid theory of the Stoner instability can be quite misleading [21], as it predicts a continuous phase transition for all values of N . A more careful treatment begins by noticing that the order parameter for $N > 2$ is a traceless hermitian matrix M belonging to the adjoint representation $N^2 - 1$ whose components are $M_{\alpha}^{\beta} \propto \sum_{\mathbf{k}} \langle [c_{\alpha}^{\dagger}(\mathbf{k}) c^{\beta}(\mathbf{k}) - \delta_{\beta}^{\alpha} c_{\alpha}^{\dagger}(\mathbf{k}) c^{\alpha}(\mathbf{k})] \rangle$. Hence, the change in the Landau free energy at the Stoner transition can be written as:

$$F - F_0 = a_2 \text{Tr } M^2 + a_3 \text{Tr } M^3 + a_4 \text{Tr } M^4 + \dots \quad (5)$$

where $a_2 \propto (F_0^m + 1)$. For $N = 2$, the second term in the right hand side of (5) vanishes because for a 2×2

traceless matrix $\text{Tr } M^3 = 0$. However, this is not so for $N > 2$, which implies that the Stoner transition is a first-order (i.e. discontinuous) transition at the mean-field level [21] (for $N = 2$ the Stoner transition becomes discontinuous at low temperatures due to fluctuation effects beyond mean field theory [101, 102]). As a consequence, close to the Stoner transition the system will exhibit metastability and phase coexistence. Furthermore, this also means that, at a quantitative level, the Pomeranchuk-Stoner criterion $F_0^m > -1$ does not provide a reliable estimate of the transition point [21]. Nevertheless, whilst qualitatively correct, the above argument assumes that the order parameter, i.e. the matrix elements of M , remain small in the neighborhood of the critical point so that keeping the lowest order terms from an expansion in M is enough to capture the transition properties. On the other hand, a direct numerical minimization of the *total* free energy which does not assume M to be small shows that this is not the case [103]. Indeed, for an ultracold gas with $\text{SU}(N > 2)$ symmetry, the Stoner transition appears to be strongly first order, although the conclusion obtained from the above free energy form remain correct only at the qualitative level.

Nevertheless, the experimental values of the gas parameter in a trap (e.g. $p_{Fa_s} \simeq 0.13$ for ^{173}Yb) are far from the critical value corresponding to the Stoner transition. Furthermore, as explained in section III C, the enhancement of the scattering length by optical means (i.e. optical Feshbach resonances), breaks $\text{SU}(N)$ symmetry and introduces large atom losses, which may complicate the applicability of the results discussed above. Yet, it may still be possible to observe a transition to a polarized (i.e. spatially segregated) state in a not too deep optical lattice, as has been recently suggested by Monte-Carlo simulations for two-component mixtures [104]. Or near half-filling in deep optical lattice, as suggested by a Gutzwiller approximation to the $\text{SU}(3)$ Hubbard model [105] and a recent generalization of Nagaoka's theorem for the $\text{SU}(N)$ Hubbard model [106].

However, although the instabilities discussed above may not be accessible in the current experimental conditions, the experimental measurement of the Landau parameters is still interesting open problem, and should provide a further confirmation that the $\text{SU}(N)$ symmetry survives many-body effects. Indeed, the lowest L Landau parameters can be obtained from the measurement of the equation of state as it was done recently for the two-component Fermi gas [107, 108] and from the measurement of the number fluctuations $\langle (N_\alpha - \langle N_\alpha \rangle)^2 \rangle$ of the different spin components [100].

B. BCS Instability and Superfluidity

Besides the Pomeranchuk instabilities, the Fermi liquid state is notoriously unstable against the formation of Cooper pairs, which is known as the BCS (after Bardeen-Cooper-Schrieffer) instability [109]. Such an instability cannot be described within the framework of Landau Fermi liquid theory because it involves

a scattering channel between Landau QPs that is neglected in Landau's theory [99, 109]. However, its importance cannot be understated since, for arbitrarily weak interactions, the Fermi liquid state is always unstable against Cooper-pair formation [110] at sufficiently low temperatures (whether such temperatures can be experimentally reached is a separate issue). The angular momentum of the Cooper pairs as well as the transition temperature depend on the details of the QP interaction, with attractive interactions typically leading to pairing in the s -wave channel, and repulsive interactions requiring higher angular momentum channels [110].

Indeed, multi-component systems exhibit a richer phase diagram of paired states [27, 29, 34–36, 111, 112] than two component systems [3, 4]. Below we focus on the case of attractive interactions and s -wave pairing. For repulsive interactions, pairing in channels other than s -wave is also possible at very low-temperatures [99, 110], which are currently beyond the experimental reach. Furthermore, d -wave pairing is also possible below half-filling (i.e. when the number of fermions per site $\lesssim 1/2$) for repulsive interactions although a weak coupling analysis [28] shows that the critical temperature rapidly decreases with N .

In order to understand the rich pairing possibilities of multi-component Fermi gases, let us recall that the s -wave order parameter of a paired state in a uniform gas is $\Delta^{\alpha\beta} \propto \sum_{\mathbf{k}} \langle c^\alpha(\mathbf{k}) c^\beta(-\mathbf{k}) \rangle$. When represented by an $N \times N$ matrix, it corresponds to an skew-symmetric matrix $\Delta^T = -\Delta$, where T means transposition. It follows that $\det \Delta = (-1)^N \det \Delta^T = (-1)^N \det \Delta$. Thus, for odd N the determinant vanishes, which implies that there is at least one zero eigenvalue. The corresponding null eigenvector v_α ($\Delta^{\alpha\beta} v_\beta = 0$) determines which component of the mixture remains *unpaired*, i.e. $c_{\text{unp}}(\mathbf{k}) = v_\alpha c^\alpha(\mathbf{k})$. This component remains in a Fermi liquid state, whereas the orthogonal components may be paired or not depending on energetic considerations [111]. In general, we can rely on Youla's decomposition [113, 114] and write $\Delta = U \tilde{\Delta} U^T$, where U is a unitary matrix and $\tilde{\Delta}$ is a skew-symmetric matrix for which only the entries $\tilde{\Delta}^{12} = \tilde{\Delta}^{34} \dots = \tilde{\Delta}^{k,k+1}$ with $k \leq N$ are non-zero while the rest vanishes. Physically, this means that it is always possible to find a basis in which component 1 pairs with 2, 3 pairs with 4, etcetera, and the system can be described in terms of $k \leq N$ Cooper-pair condensates. Such pairing states were termed diagonal pairing states by Cherng and coworkers [111]. For example for $N = 3$, two components pair whereas a third one remains unpaired. In the weak coupling limit, i.e. for $|p_F a_s| \ll 1$, the critical temperature has takes an exponential form similar to the formula obtained in the two-component mixture case: $T_c = \frac{8\epsilon_F e^{\gamma-2}}{\pi} e^{-\frac{\pi}{2p_F |a_s|}}$ [27, 29, 36], where $\epsilon_F = \frac{\hbar^2 p_F^2}{2m}$ is the Fermi energy, and $\gamma \simeq 0.5772$ Euler's constant. For the entire BEC to BCS crossover, T_c has been recently obtained by Ozawa and Baym [36], following the method of Nozières and Schmitt-Rink [115] to account for the pairing fluctuations. In the BEC limit where $p_F a_s \rightarrow 0^+$ they obtained $T_c/T_F \rightarrow 0.137$ [36].

Nevertheless, we must emphasize that the existence of $k \leq N$ Cooper pair condensates does not rely

upon the $SU(N)$ symmetry and entirely follows from Δ being a skew symmetric tensor [111, 112]. On the other hand, $SU(N)$ symmetry is important and leads to a set of Ward-Takahashi identities that are only satisfied by diagonal pairing states and not by combinations of them [111]. Moreover, the $SU(N)$ symmetry plays a crucial role in determining the number and dispersion of the Nambu-Goldstone (NG) collective modes (akin to the Anderson-Bogoliubov mode in the two-component BCS system). This is illustrated using the $SU(3)$ case in Appendix C, where it is shown that the number of NG modes is not equal to the number of broken-symmetry generators and that for N odd there are quadratically dispersion NG modes for N odd.

The existence of quadratic gapless modes and in particular a gapless unpaired component for N odd may appear to have important consequences for the superfluidity of the system, according to the Landau criterion [116]. This is because the unpaired component and the quadratically dispersing NG modes will cause dissipation when a macroscopic object moves through the fluid. However, Modawi and Leggett [27] have argued for the irrelevance of this criterion when applied to such paired states. As pointed out by these authors, the superfluid fraction at zero temperature for these systems remains finite in spite of the presence of the unpaired component.

It is also worth discussing the effects of population imbalance. Indeed, this is another aspect for which the behavior of the $N > 2$ systems noticeably deviates from the $N = 2$ case [34, 36, 111]. The reason can be understood using the following group-theoretic argument. As pointed out in the previous section, the magnetization can be represented by a hermitian traceless matrix, M . As to the pairing function, it is a complex rank-2 tensor, which can be presented by a matrix Δ . Thus, it is possible to construct a scalar invariant that couples pairing and magnetization as follows $\text{Tr} \Delta^\dagger \Delta M = -\Delta^{\alpha\beta} \Delta_{\beta\gamma}^* M_\alpha^\gamma$ (recall that $\Delta_{\alpha\beta}^\dagger = (\Delta^{\beta\alpha})^* = -(\Delta^{\alpha\beta})^*$, see Appendix A). Thus, the Ginzburg-Landau free energy reads [36, 111]:

$$F - F_0 = a_2 \text{Tr} M^2 + b_2 \text{Tr} \Delta^\dagger \Delta + c_3 \text{Tr} \Delta^\dagger \Delta M + a_3 \text{Tr} M^3 \dots \quad (6)$$

where $b_2 \propto (T - T_c)$, T_c being the critical temperature of the paired state. Hence, for $T < T_c$, unless we are dealing with a pairing state such that $\Delta^\dagger \Delta \propto \mathbf{1}$, the pairing will lead to a finite magnetization (i.e. phase segregation in a trapped system) [36, 111]. Note that this is always the case for $N = 2$ as Δ is a 2×2 skew-symmetric matrix, i.e. $\Delta^{\alpha\beta} = \Delta_0 \epsilon^{\alpha\beta}$ ($\epsilon^{12} = -\epsilon^{21} = 1$) and therefore $\Delta^\dagger \Delta = |\Delta_0|^2 \mathbf{1}$. However, this condition is not generally met for $N > 2$ and in particular, never when N is odd. The additional term in the free-energy coupling pairing and magnetization is also responsible for turning the transitions between different diagonal paired states into first-order transitions [111]. Generic phase diagrams for $N = 3, 4$ have been obtained by Cherng, Refael, and Demler in Ref. [111]. For $N = 3$, the phase diagram in entire BEC

to BCS crossover has been computed by Ozawa and Baym [36].

Finally, we should mention that attractive interactions in systems with $N > 2$ can yield phases involving more complicated bound states like trions, which would correspond to the Baryons of QCD. This possibility has been studied for three-species gases loaded in an optical lattice [35, 117].

In closing, we remark that the observation of the paired and trionic phases described above relies on the possibility of controlling the sign of the atomic interactions. Whereas this certainly is possible for both alkali atoms, using magnetic Feshbach resonances [3, 4], and AEA, using optical resonances (see section III C), both methods break the emergent unitary symmetry of the gas. Thus, how much of what has been described in this section remains valid depends on the magnitude of interaction anisotropies, which set the temperature scale above which the $SU(N)$ symmetry remains a good approximation [111].

VI. ALKALINE-EARTH ATOMS IN OPTICAL LATTICES

A. Cooling on the lattice

Although Mott insulating behavior has been experimentally demonstrated [63] (see Sec. IV), it is of great importance for the quantum simulation program to be able to cool down the optical lattice system to a regime where $k_B T < t_{gg}^2/U_{gg}$. This necessary for observing effects of magnetic exchange. Currently the achieved temperature in experiments is still in the range $t_{gg}^2/U_{gg} < k_B T < U_{gg}$. Although, this is similar to the issues encountered when studying the $SU(2)$ Hubbard model with cold alkali gases, recent investigations suggest that the large spin degeneracy present in $SU(N)$ systems can help to reach colder temperatures in fermionic AEA. In particular, Ref.[96] studied the finite-temperature Mott-insulator to Fermi gas crossover, in the regime where $k_B T > t_g$ by performing a high-temperature series expansion, together with a local density approximation assumption to deal with the external harmonic potential. It was thus shown that the final temperatures, achievable by the standard experimental protocol of adiabatically ramping up the lattice from a weakly interacting gas in a trap, can yield substantially colder Mott insulators. For example, for fixed particle numbers and fixed initial temperatures, relevant to current experiments, it was shown that increasing N from 2 to 10 can lead to Mott insulators more than a factor of five colder. Furthermore, if the initial entropy, instead of the temperature, is what is held fixed, the adiabatic procedure can lead to even better cooling for all N . The latter case seems to be experimentally relevant because the Pauli blocking effect on evaporative cooling depends on entropy, $S_i \propto T_i/T_F$, with T_F the Fermi temperature, rather than the bare temperature [63] .

The cooling can be understood as a direct consequence of the rapidly increasing entropy in a $SU(N)$

Mott insulator in the $t_g < k_B T < U_{gg}$ regime. For the $n = 1$ case, the entropy per particle grows as $S_f \propto \ln N$, since each of the N flavors is equally likely to occupy a site. For the experimentally relevant range of $N \leq 10$, the logarithm grows faster than the entropy of a quantum degenerate non-interacting gas in a 3D trap which scales for fixed initial temperature as, $S_i \propto N^{1/3}$.

The possibility of reaching colder temperatures in the regime $t_g < k_B T < U_{gg}$ by storing entropy in the nuclear spin degrees of freedom is encouraging. However, the real motivation is the exploration of exotic $SU(N)$ magnetism, which requires temperatures colder than $t_g^2/U_{gg} < t_g$ for $U_{gg} \gg t_g$. Whether or not large N can help us to reach this regime is a crucial, but at the same time challenging question. Recently, in Refs. [118, 119], Quantum Monte-Carlo methods supported by analytic [120] and DMRG (Density matrix renormalization group methods) calculations [121], showed that after adiabatically loading a weakly interacting gas into an array of one-dimensional chains, the final temperature decreases with increasing N even in the regime $k_B T < t_g^2/U_{gg}$. According to those calculations, for current initial conditions, such adiabatic loading procedure can allow us to reach temperature scales at which interesting magnetic physics happens, for example the onset of Luttinger liquid behavior and ground-state algebraic magnetic correlations [121, 122]. The cooling is a consequence of the rapid growth of the entropy with N , in the one-dimensional $SU(N)$ Heisenberg model (See Sec. VI C). At low T the entropy scales as $S_f \propto N(N-1)$ [120], even faster than its corresponding entropy in the high- T limit, where it scales as $S_f \propto \ln N$, as discussed above. The quadratic growth can be derived from the exact solution [123] and the fact that there are $N-1$ branches of elementary excitations all with the same velocity $v \propto 2\pi/N$ at small momentum. The quadratic growth of S_f with N brings the temperature of the system down with increasing N and into the region where ground-state-like correlations start to develop. This was shown in Ref. [118] by computing the relevant spin-spin correlations at finite T and comparing them to the ones expected for the ground-state from DMRG calculations [121]. Refs. [118, 119] also showed that starting from currently achievable temperatures, after adiabatic loading the gas, signatures of short range magnetic ordering could be seen in the spin structure factor for $N \geq 4$. These calculations suggest that it should be possible to explore features of $SU(N)$ quantum magnetism already in ongoing experiments with AEA.

B. The $SU(N)$ Hubbard model at weak to intermediate coupling

The $SU(N > 3)$ Hubbard model is expected to exhibit a phase diagram richer than its $SU(2)$ symmetric counter-part. In the weak to intermediate coupling limit, this phase diagram has been explored by Honerkamp and Hofstetter [28] for both the attractive and repulsive cases, and by the same authors [29] as well as Rapp *et al.* [35] for $U < 0$. Since work on the attractive case has been already reviewed in section V B,

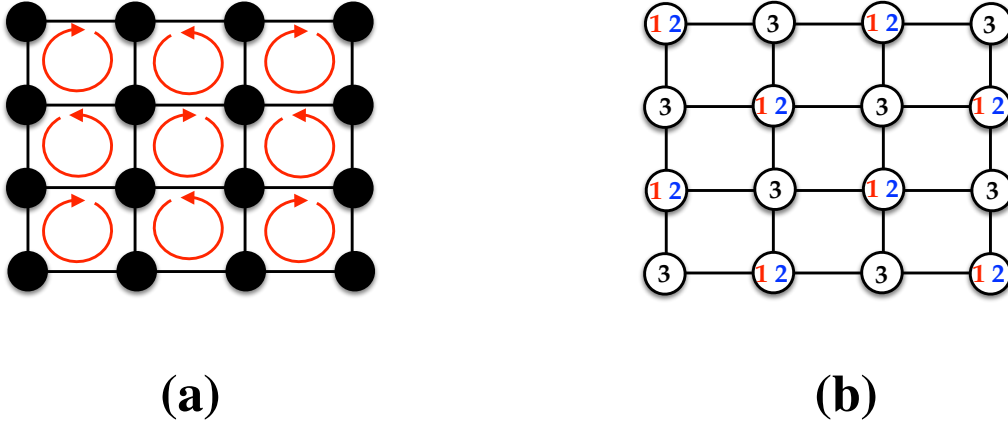


FIG. 6: Cartoon of (a) the staggered flux (SF) and (b) the flavor density-wave (FDW) phases of the SU(3) Hubbard model. The FDW phase can be regarded as a generalization of the Néel order for $N > 2$. The SF phase does not break SU(N) symmetry but breaks time-reversal invariance.

in this section we focus on the repulsive Hubbard model ($U_{gg} > 0$).

Besides the Fermi liquid phase that should be stable for $U_{gg}/t_g \lesssim 1$ and lattice fillings well away from incommensurability, the SU(N) Hubbard model with repulsive interactions can display various types of ordered phases. Some of those phases break the lattice translation symmetry and may or may not break the SU(N) symmetry at the same time. In this respect, they are different from the phases discussed in section V, whose order parameters have no spatial dependence (for a uniform system) because these phases do not spontaneously break translational invariance.

Perhaps the most spectacular example of the above type of phenomena is a phase that breaks lattice translation symmetry without breaking SU(N), known as the staggered flux (SF) phase (Fig. 6a). This phase was obtained as a mean-field solution of the Hubbard model shortly after the latter gained relevance as the minimal model for the high- T_c cuprate superconductors [44, 45]. It has been postulated as candidate to explain the anomalous pseudo-gap phase of these materials [124]. The mean-field solution obtained by Marston and Affleck [44, 45] is the exact ground state of the SU(N) Hubbard model for a 2D half-filled lattice (filling fraction $n = \langle n_i \rangle = N/2$) in the $N \rightarrow +\infty$ limit [44, 45]. Therefore, it is expected [21, 28] that it can be realized using ultracold gases as values of N can be as large as 10 using ^{87}Sr (Table I). However, as pointed out by Honerkamp and Hofstetter [28], at values of $N \lesssim 6$, a functional renormalization-group analysis (see also [105], for a recent variational study) shows that another phase, known as a flavor density wave (FDW) phase (Fig. 6 a) is favored over the SF phase. Like the SF phase, the FDW phase also breaks lattice translational symmetry. However, unlike the SF phase, it also breaks SU(N) symmetry. According to Ref. [28], ^{173}Yb is on the borderline for the stabilization of the SF phase, whereas ^{87}Sr is probably a better candidate. It also worth mentioning that the SF phase is characterized by an Ising order parameter

which is the direction of the angular momentum associated with the fermion current in each plaquette of the 2D square lattice. Thus, in 2D, the long-range SF order is stable at finite temperatures, which may facilitate its observation using ultracold atoms.

However, one major challenge for the observation of these phases is, not only their relatively low ordering temperatures (compared to t_g), but the requirement of a lattice fillings at or near the half-filled lattice (*i.e.* $n = \langle n_i \rangle \simeq N/2$). For large N this requires a relatively tightly confinement trapping potential so that large n plateaux can form at the center of the trap [21]. However, under such circumstances, it is not clear how stable such the lattice system would be against inelastic losses. For instance, using ^{173}Yb , a half-filled insulating plateau containing $N/2 = 3$ atoms per site can be reached at the center of the trap [21]. However, the existence of such plateau makes the system very susceptible to three-body recombination and the unwanted heating effects associated with it. A precise experimental determination of the lifetime of a high-filling optical lattice for common AEA is in order. Furthermore, on the theory side, not much is known about how such phases, and in particular the SF phase can be detected in the optical lattice setup.

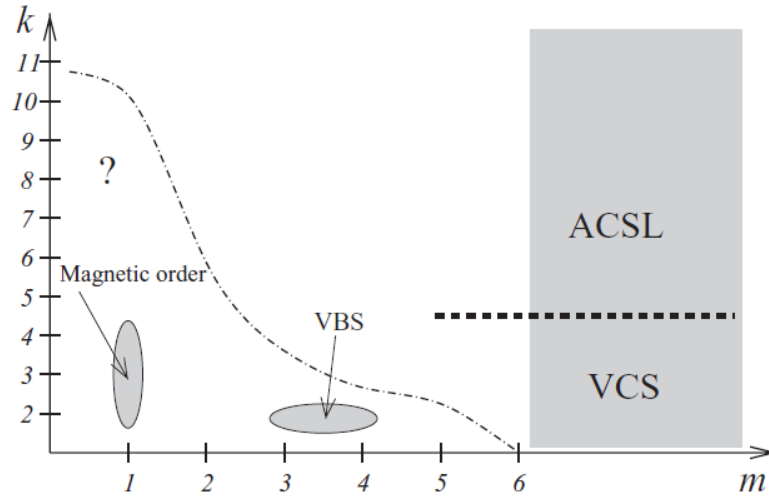


FIG. 7: Phase diagram of the $SU(N)$ Heisenberg model in two dimensions on the square lattice with $N = mk$, taken from Ref.[125]. m is the number of fermions per site, and k is the number of sites needed to form a singlet. Regions where there is substantial evidence for a given ground state, or where the ground state is known, are shaded. The Abelian chiral spin liquid (ACSL) and valence cluster state (VCS) regions on the right are established by large- N analysis; the boundary between these regions in large N is shown by a dashed line. For $k = 2, m = 1$, the Neel state is the well-known ground state. There is also evidence for magnetic order at $k = 3, m = 1$ [126] and $k = 4, m = 1$ [127]. Valence-bond solid (VBS) order was found for $k = 2$ and $m = 3, 4$ [128]. The dashed-dotted line separates the range of parameters beyond the reach of current experiments (above and to the right of the line) and the range within the reach of the experiments (below and to the left of the line). The experimentally relevant part of the phase diagram with the greatest potential for novel ground states, in particular, the Abelian chiral spin liquid, is indicated with a question mark.

C. Strong coupling limit: The $SU(N)$ Heisenberg model

As we have discussed already in section IV, when AEA in their ground electronic state are loaded into a deep optical lattice they provide us with an accurate realization of the $SU(N)$ Hubbard model (see Eq. 2). In the limit of large U_{gg}/t_g and for integer filling fractions the system becomes a Mott insulator. In this regime the motion of the particles only takes place virtually, since adding or removing a particle at a giving lattice site costs energy, and the Hamiltonian reduces to an effective spin Hamiltonian. Assuming a translational invariant system for simplicity (setting $V = 0$), the effective model obtained by second order degenerate perturbation theory is the $SU(N)$ Heisenberg model [22]

$$H = \frac{2t_g^2}{U_{gg}} \sum_{\langle i,j \rangle} S_\alpha^\beta(i) S_\beta^\alpha(j), \quad (7)$$

where the spin operators $S_\alpha^\beta(i) = c_{\alpha,i}^\dagger c_i^\beta$ which satisfy the $SU(N)$ algebra $[S_\alpha^\beta(i), S_\gamma^\delta(j)] = \delta_{ij}(\delta_{\beta\gamma} S_\alpha^\delta - \delta_{\alpha\delta} S_\beta^\gamma)$ (see Appendix A).

Like the Hubbard model reviewed above, the $SU(N)$ Heisenberg model can also display a rich phase diagram. The phases depend on N , the filling fraction $n = \langle n_i \rangle$, dimensionality and lattice geometry. The parameter $k \equiv N/n$, chosen to be an integer greater than unity, plays a key role in the analysis of the phase diagram: k is the minimum number of sites needed to form a $SU(N)$ singlet. The one dimensional chain with $n = 1$ admits an exact solution for all N [123] and its phase diagram is well understood. Nevertheless, the phase diagram of the 2D model is complex and remains unknown to a great extent. The phase diagram predicted in Refs. [37, 125] for a square lattice is shown in Fig. 7. There m labels the filling fraction (i.e $m = n$). The dashed-dotted line separates the range of parameters beyond the reach of current experiments (above and to the right of the line) and the range within the reach of the experiments (below and to the left of the line covering the region $N \leq 10$ and $n \leq 5$). The predictions for the quantum phases, based on a large- N expansion and thus valid in the limit $N \gg 1$ for k finite, have been shaded, as well as regions where the ground state is known.

The known regions correspond to the well established $N = 2$ and $n = 1$ or $k = 2$ case, where anti-ferromagnetic long range order is favored, and the ground state is the so called Neel state. The generic case $k = 2$ shares with $SU(2)$ the crucial property that two adjacent spins can form an $SU(N)$ singlet, and has been studied extensively as a large- N generalization of $SU(2)$ magnetism [44–46, 129]. Those studies found that under very general conditions in the large- N limit, the ground state is non-magnetic and spontaneously breaks lattice symmetries. It is formed by two-site singlets and referred to as a valence-bond solid (VBS). Quantum Monte Carlo simulations done for $N = 3, 4$ have confirmed that the ground state

remains a VBS even at finite N . Numerical studies of the cases $N = 3, 4$ but $n = 1$ (or $k = 3, 4$) in a square lattice [126, 127] on the contrary provide strong evidence of magnetically ordered ground states.

The large- N expansion predicts two different ground states depending on k : a valence cluster state (VCS) formed by tiling the lattice with multisite singlet clusters for $k < 5$ and an Abelian chiral spin liquid (ACSL), which is a spin-system analog of a Fractional Quantum Hall state [38, 39, 130], for $k \geq 5$. A VCS is non-magnetic and breaks lattice symmetries. The ACSL spontaneously breaks parity and time-reversal symmetry, supports excitations with fractional quantum numbers and statistics, and has gapless chiral edge states that carry spin.

Although we have focused our analysis of the phase diagram of the $SU(N)$ -Heisenberg model on a square lattice, which is the simplest to generate in experiments, it is important to mention that it is expected to be even richer in more generic lattice geometries. For example numerical investigations of the $SU(3)$ -Heisenberg model in a triangular lattice predict a perfectly ordered three-sublattice state [131]. On a honeycomb lattice, the $SU(3)$ case has been shown to have a dimerized, magnetically ordered state [132–134], and it has been also predicted that the $SU(6)$ case becomes a ACSL using a large $1/N$ expansion [135, 136]. Whether or not the ACSL remains the ground state in the experimentally relevant part of the phase diagram, $k = N$ and $n = 1$ is not unknown and needs to be validated by experiments.

VII. OTHER EXOTICA: PHYSICS BEYOND THE $SU(N)$ HEISENBERG MODEL

In this section we present an overview of some of the recently proposed exciting physics that near term AEA experiments could explore. Most of those proposals take advantage of the long life time of the 3P_0 state, in addition to the $SU(N)$ symmetry in the nuclear spin levels.

A. Orbital magnetism

The possibility to independently manipulate the 1S_0 and 3P_0 states by laser light and therefore to construct identical or different optical lattices for the two states [137] allows for the simulation of two-orbital- $SU(N)$ Hamiltonians which rely on the interplay of charge, spin and orbital degrees of freedom. The electronic clock states play the role of the orbital degree of freedom and the corresponding nuclear spins provide the spin degree of freedom. The investigation of orbital physics using alkali-metal atoms has of course also been considered. For example, a natural way to add orbital degrees of freedom is to encode the spin in their internal hyperfine degrees of freedom, and the orbital degree of freedom in different lattice bands. However, one important limitation of this approach is that the occupation of excited lattice bands is,

at best, metastable [4]. Spin mixtures in alkali atoms in which the orbital degree of freedom is encoded in different type of atoms has been thought as an alternative to explore orbital physics without the necessity of populating higher bands. In this case one can easily impose an optical lattice which acts differently on the two species of atoms owing to their different optical properties. However, in this case atom distinguishability only gives rise to pure density-density interactions without direct spin interconversion. The emulation of orbital physics by using the lowest band orbitals of independent optical lattice felt by the 1S_0 and 3P_0 states does not have any of the metastability issues of higher bands, and allows also for nuclear spin flip processes. Collisional relaxation of the electronic excited states must however be considered [138, 139]. A possible way to deal with it is to work in the regime where there is only one 3P_0 atom per lattice site.

The implementation of the two-band $SU(N)$ Hubbard model with alkaline earth atoms opens untapped opportunities [22, 140, 141], including the implementation of a $SU(N)$ generalization of the $SU(2)$ -Kondo lattice model (one of the canonical models used to study strongly correlated electron systems, such as manganese oxide perovskites [142] and rare-earth and actinide compounds classed as heavy-fermion materials [143]) and a $SU(N)$ generalization of the $N=2$ Kugel–Khomskii Hamiltonian (used to model the spinorbital interactions in transition-metal oxides with the perovskite structure [144]). Just recently it was also pointed out that a $SU(N)$ -Mott insulator with one ground state atoms and one excited state atoms on each site of a square lattice is likely to realize a non-Abelian Chiral spin liquid with a quantum statistics sufficient for universal quantum computations [125, 145]. Note that other non-Abelian states such as the fractional quantum Hall state at the filling fraction $5/2$ [146, 147] or a variety of setups involving Majorana fermions [148] are not rich enough to support universal quantum computation [149]. Recent numerical studies of the phase diagram of the $SU(4)$ Kugel–Khomskii model in a honeycomb lattice predict a quantum spin-orbital liquid ground state [136].

B. Artificial Gauge fields

Atoms are neutral particles and thus they do not experience Lorentz forces in the presence of electromagnetic fields. Recently, it has been demonstrated that when a neutral atom is illuminated with properly designed laser fields, its center-of-mass motion can mimic the dynamics of a charged particle. This is the basis of the so called artificial (synthetic) Gauge fields for atoms [150]. Although there has been important advances in implementing those ideas in alkali atoms by coupling their internal or motional states with laser light [151–156] spontaneous emission of the excited levels always imposes limitations. AEA have been pointed out to be ideal for synthetic gauge field implementation [157] thanks to the long lifetime of the excited state, its reduced spontaneous emission rate and the possibility of generating anti-magic lattice

potentials for the clock states –the clock states feel exactly the same lattice but with an opposite sign–. The latter has been shown also to facilitate the implementation the so-called optical flux lattices [158, 159]. In addition the large number of decoupled nuclear spin degrees of freedom could facilitate the implementation of $SU(N)$ non-Abelian gauge fields and spin-orbit Hamiltonians exhibiting rich quantum dynamics and connections to high energy physics [160, 161]. For the use of AEA for artificial gauge field implementation however, collisional relaxation of the electronic excite states could impose important limitations and must be considered [138, 139].

VIII. ATOM-LIGHT HYBRID SYSTEMS AND MANY-BODY PHYSICS IN OPTICAL CLOCKS

Recent advances in modern precision laser spectroscopy, with record levels of stability and residual laser drift less than mHz/s [11–13, 162] are crucial developments that are allowing us to deal with AEA clocks operated at a very different conditions than those ones dealt with just few years ago. The level of energy resolution achievable in current atomic clocks is now providing the required capability to systematically spectrally resolve the complex excitation spectrum of an interacting many-body system. This was certainly not the case in prior clock experiments where interaction effects were subdominant. Optical atomic clocks operating with AEA are thus becoming a new laboratory for the exploration of non-equilibrium many-body phenomena with capabilities not foreseen before[139, 163–169].

Moreover the combination of this new regime of ultrastable atomic dipoles with optical cavities, is predicted to become a pathway for realization of exotic states of matter and light. The idea here is to make the leap to using light to mediate interactions between atoms, impose coherence, and/or directly drive dynamics through strong coupling to matter [170, 171]. The long-lived dipoles will allow coherent interaction of many atoms with a single optical cavity mode over an extraordinarily long time, generating strong correlations. Experiments performed using Raman transitions in alkali vapors to mimic the ultrastable alkaline-earth dipoles, which have observed superradiant behavior maintained with less than one photon in the cavity, provide first principle demonstration of this outstanding capability[172].

IX. SUMMARY AND OUTLOOK

Much has been achieved since the first time alkaline-earth atom gases were brought to quantum degeneracy. The creation of Bose-Einstein condensates rapidly led to the production of quantum degenerate Fermi gases. The latter, as we have discussed above, exhibit an emergent $SU(N)$ symmetry, which makes of these gases rather unique many-body systems. Since this fact was pointed out, the field has evolved

rapidly leading to the creation of a $SU(6)$ Mott insulator [63] and, very recently, to the realization of arrays of one-dimensional and quantum degenerate ultracold ^{173}Yb gases [20]. These experiments have also demonstrated that, thanks to the large entropy that can be stored in the nuclear spin degree of freedom of the AEA gases, there is much room for improvement in the quest for cooling down AEA to lower and lower temperatures (entropies) using conventional methods such as sympathetic cooling and adiabatically loading into the lattice.

We point out nevertheless that, regardless all the great progress, what has been experimentally demonstrated so far [20, 63] is just fairly interesting physics related to the “charge” degrees of freedom. The real challenge associated with the observation of quantum magnetism and many of the other exotic phases that have been described in previous sections still needs to be overcome. Those phases should become stable to thermal fluctuations well below the hopping temperature scale $\sim t_g/k_B$, and typically at $k_B T \ll t_g^2/U_{gg}$ for the Hubbard model of section IV. As we have emphasized above, we expect that the large spectral degeneracies introduced by the enlarged $SU(N)$ symmetry will bring about new phenomena which have no counterpart in the two-component systems. Some hints of these differences have already shown up in the experiments [20, 63], but there is more to come if we can find a way to remove the entropy from the nuclear degree of freedom. This is a challenge that will require new ideas, perhaps different from those applicable ultracold gases of alkali atoms.

As we have seen, turning other parameters like the interactions in AEA also requires using different methods like optical Feshbach resonances. Unfortunately, the latter generally spoils the emergent $SU(N)$ symmetry that makes these gases so special. New ideas are also required in this regard. And if an efficient and versatile way is found to tune the interactions while respecting the $SU(N)$ symmetry, this will open the door to the exploration of superfluidity and ferromagnetism in these systems. The landscape associated with phases, as we have described in section V will be rather rich, exhibiting interesting excitations and topological defects as well as discontinuous phase transitions between them. Those can lead to spectacular phase segregation patterns (i.e. domains) in a trap. On a different but complementary direction, although the potential use of the exquisite precision of optical lattice clocks to probe AEA manybody physics has started, there is still lots of room for improvement.

But in spite of the limitations of the present, it is important to emphasize that seeds for a bright future of the field have been already planted. We strongly believe that there is much more to come, and hopefully many serendipitous discoveries are waiting for us. Some of such discoveries may come in the form of new phases of matter, which do not fit into the relatively narrow framework that we have outlined in this article. Or they may come by exploring non-equilibrium phenomena with AEA gases. Indeed, this is a field that, compared to what has been already achieved using alkali gases, remains largely unexplored at the time of

writing this article. And as it happens for equilibrium phenomena, we have a new parameter to play with, namely N (or $1/N$, depending on the point of view). In conclusion, we hope that this review will become the starting point for many of the bold minds wanting to explore these fascinating new systems.

X. ACKNOWLEDGMENTS

We thank Karlo Penc, Sungkit Yip, and Yoshihiro Takahashi for useful comments on the manuscript and discussions. MAC acknowledges support from NSC and NTHU (Taiwan). AMR acknowledges funding from NIST, JILA-NSF-PFC-1125844, NSF-PIF, ARO, ARO-DARPA-OLE, and AFOSR.

Appendix A: Brief Digest of $SU(N)$ Group Theory

In this Appendix we briefly review the most important facts about the special unitary group $SU(N)$. We begin by defining it. To this end, let us first introduce a N -dimensional linear space of complex vectors denoted as $\psi^T = (\psi^1, \dots, \psi^N)$, where T means transpose, and the components ψ^α ($\alpha = 1, \dots, N$) are complex numbers. In this linear space, we define the scalar product between two vectors ψ and χ as $\langle \psi | \chi \rangle = \sum_\alpha (\psi^\alpha)^* \chi^\alpha$. In order to lighten the notation, we introduce the dual of the vector ψ defined by $\psi_\alpha = (\psi^\alpha)^*$. This allows to write $\langle \psi | \chi \rangle = \psi_\alpha \chi^\alpha$, where repeated upper and lower indices are to be summed over, unless stated otherwise. Finally, the norm of $|\psi\rangle$ can be defined as $\sqrt{\langle \psi | \psi \rangle} = \sqrt{\psi_\alpha \psi^\alpha}$. Let next us consider the linear transformation

$$\tilde{\psi}^\alpha = U^\alpha_\beta \psi^\beta. \quad (\text{A1})$$

Hence, the dual $\tilde{\psi}_\alpha = (\tilde{\psi}^\alpha)^* = (\psi^\beta)^* (U^\beta_\alpha)^* = \psi_\beta (U^\dagger)_\alpha^\beta$, where we have employed that $(U^\dagger)_\beta^\alpha = (U^\beta_\alpha)^*$, where U^\dagger is the hermitian conjugate of the matrix U .

We are now ready to define the $SU(N)$ group as the set of *linear* transformations that preserve the norm of vectors. Mathematically, $\langle \tilde{\psi} | \tilde{\psi} \rangle = \langle \psi | \psi \rangle$. Hence, using (A1) leads to:

$$\langle \tilde{\psi} | \tilde{\psi} \rangle = \psi_\alpha (U^\dagger)_\beta^\alpha U^\beta_\gamma \psi^\gamma = \psi_\alpha \psi^\alpha = \langle \psi | \psi \rangle \quad (\text{A2})$$

which, for arbitrary ψ , is only possible provided $(U^\dagger)_\beta^\alpha U^\beta_\gamma = \delta^\alpha_\gamma$, that is, in matrix notation:

$$U^\dagger U = U U^\dagger = \mathbf{1}, \quad (\text{A3})$$

where $\mathbf{1}$ is the unit matrix. Hence, $U^{-1} = U^\dagger$, or, in other words, U is a *unitary* matrix. Furthermore, it also follows that $\det[U^\dagger U] = \det \mathbf{1} = 1$, which implies that $|\det(U)|^2 = 1$. If U belongs to $SU(N)$, then $\det(U) = \epsilon_{\alpha_1 \dots \alpha_N} U_1^{\alpha_1} \dots U_N^{\alpha_N} = 1$, which generalizes to $\epsilon_{\alpha_1 \dots \alpha_N} U_{\beta_1}^{\alpha_1} \dots U_{\beta_N}^{\alpha_N} = \epsilon_{\beta_1 \dots \beta_N}$. The vector and its dual define the two fundamental irreducible representations of $SU(N)$, which are denoted as N and \bar{N} , respectively. We can consider tensors with upper and lower indices which transform as products of these two fundamental representations. For instance, $\varphi^{\alpha\beta}$ belongs to the $N \times N$ tensor which transforms as $\psi^\alpha \chi^\beta$. The tensor φ_β^α belongs to $N \otimes \bar{N}$ representation transforming as $\psi^\alpha \chi_\beta$. It is worth noting that the transformation properties of the tensors respect the permutation symmetries of their indices. Thus, for $\varphi^{(\alpha\beta)} = \varphi^{\alpha\beta} = \varphi^{\beta\alpha}$ ($\varphi^{[\alpha\beta]} = \varphi^{\alpha\beta} = -\varphi^{\beta\alpha}$) a(n) (anti-)symmetric tensor, the transformed tensor $\tilde{\varphi}^{\alpha\beta} = U_\gamma^\alpha U_\delta^\beta \varphi^{\gamma\delta}$ is also (anti-)symmetric. Hence, since the tensor $\varphi^{\alpha\beta} = \varphi^{[\alpha\beta]} + \varphi^{(\alpha\beta)}$, where (\dots) stands for symmetrization of the indices and $[\dots]$ for symmetrization, we have that the representation $N \otimes N$ is reduced to $N(N-1)/2 \oplus N(N+1)/2$. Furthermore, an $SU(N)$ transformation respects the trace of a tensor (the latter being understood as the result of contracting an upper and a lower index). Hence, for instance, $\varphi_\beta^\alpha = \frac{1}{N} \varphi_\alpha^\alpha \delta_\beta^\alpha + \left(\varphi_\beta^\alpha - \frac{1}{N} \varphi_\alpha^\alpha \right)$, that is, $N \otimes \bar{N} = \mathbf{1} \oplus N^2 - 1$.

Finally, let us consider the linear transformations in the neighborhood of the unit element of the group (i.e. $\mathbf{1}$). For $N = 2$, $SU(2) \simeq O(3)$, the rotation group, and for this group it is known that any finite rotation can be obtained as the product of an infinite set of infinitesimal rotations. The latter differ from unity $\mathbf{1}$ by an infinitesimal amount, i.e. $U = \mathbf{1} + i\epsilon T$, where $\epsilon \ll 1$ is a real parameter and T is a matrix whose properties we determine in what follows. From (A3) it follows that $U^\dagger U = (\mathbf{1} - i\epsilon T^\dagger)(\mathbf{1} + i\epsilon T) = \mathbf{1} - i\epsilon(T^\dagger - T) + O(\epsilon^2) = \mathbf{1}$, that is,

$$T^\dagger = T. \quad (\text{A4})$$

Moreover, the unit determinant condition requires that $1 = \det U = \det (\mathbf{1} + i\epsilon T) = \text{tr} \exp [\ln(\mathbf{1} + i\epsilon T)] = 1 + i\epsilon \text{tr} T$, where we have employed the identity $\det A = \text{tr} \exp [\ln A]$. Therefore, $\text{tr} T = 0$, thus, the $N \times N$ matrices T are hermitian (see (A4)) and *traceless*. When expressed in terms of the matrix components, (A4) reads $(T_\alpha^\beta)^* = T_\beta^\alpha$. In other words, the diagonal elements of T are real, and the $N(N-1)/2$ upper and lower diagonal are the complex conjugate to each other. Hence, it follows that T depends only on $2 \times N(N-1)/2 + N = N^2$ real parameters. The traceless condition imposes a further constraint, which yields $N^2 - 1$ for the number of independent T matrices, which are denoted as T^a , with $a = 1, \dots, N^2 - 1$. Thus, a general infinitesimal $SU(N)$ transformation can be written as $U = \mathbf{1} + i \sum_a \epsilon_a T^a$, where $\epsilon_a \ll 1$ are $N^2 - 1$ *real* numbers. For $N = 2$, there are $2^2 - 1 = 3$ matrices proportional to the Pauli matrices $T^a = \frac{1}{2} \sigma^a$, $a = x, y, z$. The latter satisfy the angular momentum algebra

$[T^a, T^b] = i\epsilon_c^{ab}T^c$, where ϵ_c^{ab} is the fully anti-symmetric Levi-Civita symbol. This is an example of a *Lie* algebra. For $SU(N > 2)$, the Lie algebra is characterized by a set of structure constants f_c^{ab} different from ϵ_c^{ab} :

$$[T^a, T^b] = if_c^{ab}T^c, \quad (\text{A5})$$

The $N^2 - 1$, $N \times N$ traceless hermitian matrices, T^a , are the generators of the Lie algebra. Furthermore, they also provide a basis for the linear space of $N \times N$ *traceless* hermitian matrices. Among them, we can distinguish $N - 1$ that are diagonal (like $T^3 = \sigma^z/2$ for $SU(2)$), which form a set known as the Cartan basis. A representation for Cartan basis matrices is $T_3 = \frac{1}{2}\text{diag}(1, -1, 0, \dots, 0)$, $T_8 = \frac{1}{\sqrt{12}}\text{diag}(1, 1, -2, 0, \dots, 0), \dots$, $T^{r^2-1} = \frac{1}{\sqrt{2(2r-1)}}(1, 1, 1, \dots, -r, \dots, 0)$, for $r = 2, \dots, N$. The other matrices are chosen hermitian and non-diagonal and contain a single non-vanishing element equal to either $1/\sqrt{2}$ or $i/\sqrt{2}$. This basis is conveniently normalized so that $\text{Tr } T^a T^b = \frac{1}{2}\delta^{ab}$. Another convenient basis for $U(3) = U(1) \times SU(3)$ is provided by the projection operators $X_\beta^\alpha = |\alpha\rangle\langle\beta|$, where $a, b = 1, \dots, N$. In this basis, the Lie algebra takes a very simple form:

$$[X_\beta^\alpha, X_\delta^\gamma] = \delta_\gamma^\beta X_\delta^\alpha - \delta_\delta^\alpha X_\beta^\gamma. \quad (\text{A6})$$

Furthermore, $n = X_\alpha^\alpha$ commutes with all the generators X_β^α , and corresponds to the generator of the $U(1)$ subgroup in $U(3) = U(1) \times SU(3)$. Note that the non-diagonal generators ($\alpha \neq \beta$) are not hermitian, whereas the diagonal ones are not traceless. However, this basis has the advantage that it can be readily represented in second quantization: Let c_α transforms according to the N irrep, and c_α^\dagger transform according to \bar{N} , then $X_\beta^\alpha = c_\beta^\dagger c^\alpha$, provided $n = c_\alpha^\dagger c^\alpha = 1$.

Appendix B: Fermi Liquid Parameters

We can exploit the $SU(N)$ symmetry and write the Landau QP occupation and the Landau function as follows [21]:

$$\delta n_\beta^\alpha(\mathbf{p}) = \frac{1}{N}\delta\rho_c(\mathbf{p})\delta_\beta^\alpha + \sum_{a=1}^{N^2-1} m_a(\mathbf{p}) (T^a)_\beta^\alpha, \quad (\text{B1})$$

$$f_{\alpha\gamma}^{\beta\delta}(\mathbf{p}, \mathbf{p}') = f^\rho(\mathbf{p}, \mathbf{p}')\delta_\beta^\alpha\delta_\delta^\gamma + 2f^m(\mathbf{p}, \mathbf{p}') \sum_{a=1}^{N^2-1} (T^a)_\beta^\alpha (T^a)_\delta^\gamma, \quad (\text{B2})$$

where we have exploited the fact that $\delta n_\beta^\alpha(\mathbf{p})$ is a $N \times N$ (hermitian) density matrix which can be split into a trace $[\delta \rho_c(\mathbf{p}) = \delta n_\alpha^\alpha(\mathbf{p})]$, which describes fluctuations in the total QP number, and a traceless part. The latter can be conveniently expanded in terms of the generators of the $SU(N)$ algebra (see Appendix A) and describes the nuclear spin fluctuations. In group theoretic language, $\delta n_\beta^\alpha(\mathbf{p})$ is a rank-2 tensor in the (reducible) $N \otimes \bar{N} = 1 \oplus N^2 - 1$ representation (see Appendix A for definitions). Likewise, the fourth rank tensor of Landau functions belongs to the (reducible) representation $N \otimes \bar{N} \otimes N \otimes \bar{N} = 1 \oplus 1 + \text{non-scalar representations}$, and therefore it can be parametrized in terms of two scalar functions as in Eq. (B2). Because the QP are only well-defined excitations in the neighborhood of the FS (otherwise the strongly scatter each other), for $|\mathbf{p}| = |\mathbf{p}'| \approx p_F$, rotational invariance requires that the Landau functions depend only on $\cos \theta = \mathbf{p} \cdot \mathbf{p}' / p_F^2$. Thus, it is conventional [98] to express the Landau functions $f^\rho(\cos \theta)$ and $f^m(\cos \theta)$ in terms the dimensionless Landau parameters $F_L^{\rho,m}$:

$$f^\rho(\cos \theta) = [N \times N^0(\mu)]^{-1} \sum_{L=0}^{+\infty} F_L^{\rho,m} P_L(\cos \theta), \quad (\text{B3})$$

$$f^m(\cos \theta) = [N^0(\mu)]^{-1} \sum_{L=0}^{+\infty} F_L^m P_L(\cos \theta), \quad (\text{B4})$$

where $N^0(\mu) = p_F m^* / (\pi^2 \hbar^2)$ is the QP density of states per spin at the Fermi level and $P_L(\cos \theta)$ are the Legendre polynomials of order L .

Appendix C: Nambu-Goldstone modes of $SU(N)$ superfluids

To illustrate this point, let us consider the $SU(N = 3)$ case [29, 34, 112]. The order parameter is a rank-2 tensor that transforms according to the $\bar{3}$ irreducible representation of $SU(3)$ (recall that $3 \otimes 3 = \bar{3} \oplus 6$, where $\bar{3}$ is the anti-symmetric representation, see Appendix A). This is made apparent by introducing the (complex) spinor Φ whose components are $\Phi_\alpha = \epsilon_{\alpha\beta\gamma} \Delta^{\beta\gamma}$, where $\epsilon_{\alpha\beta\gamma}$ is the fully anti-symmetric Levi-Civita symbol. Applying Youla's decomposition, we can use a Gauge for which $\Delta^{12} = \phi_0 \neq 0$ and the other components are zero, which means that we can always choose $\Phi = (0, 0, \phi_0)$. Consequently, the little group that is, the symmetry group that leaves the order parameter invariant is $SU(2) \times U(1)$, where $SU(2)$ acts upon the first two components of Φ whereas the $U(1)$ group acts on the phase of the third (non-zero) component. Thus, the little group contains $3 + 1 = 4$ generators, meaning in $U(3) = U(1) \times SU(3)$ (9 generators) there are $9 - 4 = 5$ broken-symmetry generators [29]. However, in non-relativistic systems, the number of NG modes is not equal to the number of broken symmetry generators (see e.g. Ref. [173] and references therein). Qualitatively, this can be understood by writing down an effective Lagrangian for the

order parameter spinor field $\Phi(\mathbf{r})$. Besides the U(3) symmetry, the latter is constrained by space rotation invariance, which leads to

$$\mathcal{L} = i\Phi^\dagger(\mathbf{r}, t)\partial_t\Phi(\mathbf{r}, t) - \frac{K_1}{2}\nabla\Phi^\dagger(\mathbf{r}, t) \cdot \nabla\Phi(\mathbf{r}, t) - V(\Phi^\dagger\Phi) + \dots \quad (\text{C1})$$

where K_1 is a constant, the potential $V(\Phi^\dagger\Phi)$ has a minimum for $\Phi^\dagger\Phi = \phi_0^2$, e.g. $V = \frac{\lambda}{2}(\Phi^\dagger\Phi - \phi_0^2)^2$ (we take ϕ_0 real without loss of generality), and the dots stand for higher order gradient terms. Note that in a relativistic (i.e. Lorentz-invariant) or in a particle-hole symmetric theory, the first term in the right-hand side of Eq. (C1) would be forbidden and should be replaced by $\sim \partial_t\Phi^\dagger\partial_t\Phi$. For such theories, the number of NG modes equals the number of broken symmetry generators [173]. However, in the non-relativistic case, as we shall see next, this term is responsible for a dramatic change in the number and long-wave length dispersion of the NG modes. If we parameterize the small fluctuations about the minimum as $\Phi(\mathbf{r}, t) = (\phi_1(\mathbf{r}, t), \phi_2(\mathbf{r}, t), [\phi_0 + \delta\rho_3(\mathbf{r}, t)]e^{i\theta(\mathbf{r}, t)})$, it can be seen that the linearized equations of motion for $\theta(\mathbf{r}, t)$ and $\phi_{1,2}(\mathbf{r}, t)$ imply that the phase (θ) NG mode has linear dispersion, i.e $\omega \propto q$ for $q \rightarrow 0$. However, the $\phi_{1,2}$ NG modes disperse quadratically, i.e. $\omega \propto q^2$ as $q \rightarrow 0$. Furthermore, the number of NG modes is three, which is different from the number of Broken symmetry generators (= 5) because, upon quantization, the fields ϕ_1^*, ϕ_2^* and ϕ_1, ϕ_2 cannot be treated as independent degrees of freedom as they correspond to the creation and annihilation of the same eigenmode.[34, 112]. Another lesson from this example is that quadratic modes correspond to fluctuations in the pairing function of the two paired components with unpaired one, i.e. $\Phi_1 = \Delta_{23}$ and $\Phi_2 = \Delta_{13}$. This is because, in the linearized equations that follow from (C1), ϕ_1, ϕ_2 are not coupled to each other and to ϕ_3 . However, $\delta\phi_3 = \phi_3 - \phi_0 \sim \delta\rho_3 e^{i\theta}$, and $\delta\phi_3^* \sim \delta\rho_3 e^{-i\theta}$ are coupled, which leads to the linear dispersion for θ . This observation also generalizes to larger odd values of $N = 5, 7, \dots$, implying that for $N = 5$ there are four quadratic NG modes, etc. The quadratic coupling of the NG modes involving the unpaired component can also be explained using Gauge invariance arguments [112]. For even values of N , the NG modes disperse linearly at small q [112].

-
- [1] R. P. Feynman, International Journal of Theoretical Physics **21**, 467 (1982).
 - [2] R. P. Feynman, A. J. G. Hey, and R. W. Allen, *Feynman lectures on computation* (Perseus Books, Cambridge, Mass., 1999).
 - [3] S. Giorgini, L. P. Pitaevskii, and S. Stringari, Rev. Mod. Phys. **80**, 1215 (2008).
 - [4] I. Bloch, J. Dalibard, and W. Zwerger, Rev. Mod. Phys. **80**, 885 (2008).
 - [5] D. Jaksch, C. Bruder, J. I. Cirac, C. W. Gardiner, and P. Zoller, Phys. Rev. Lett. **81**, 3108 (1998).
 - [6] M. Greiner, O. Mandel, T. Esslinger, T. W. Hansch, and I. Bloch, Nature **415**, 39 (2002).

- [7] R. Jordens, N. Strohmaier, K. Gunther, H. Moritz, and T. Esslinger, *Nature* **455**, 204 (2008).
- [8] U. Schneider, L. Hackermuller, S. Will, T. Best, I. Bloch, T. A. Costi, R. W. Helmes, D. Rasch, and A. Rosch, *Science* **322**, 1520 (2008).
- [9] A. Derevianko and H. Katori, *Reviews of Modern Physics* **83**, 331 (2011).
- [10] A. D. Ludlow, T. Zelevinsky, G. K. Campbell, S. Blatt, M. M. Boyd, M. H. G. de Miranda, M. J. Martin, J. W. Thomsen, S. M. Foreman, J. Ye, et al., *Science* **319**, 1805 (2008).
- [11] T. L. Nicholson, M. J. Martin, J. R. Williams, B. J. Bloom, M. Bishof, M. D. Swallows, S. L. Campbell, and J. Ye, *Phys. Rev. Lett.* **109**, 230801 (2012).
- [12] N. Hinkley, J. A. Sherman, N. B. Phillips, M. Schioppo, N. D. Lemke, K. Beloy, M. Pizzocaro, C. W. Oates, and A. D. Ludlow, *Science* **341**, 1215 (2013).
- [13] B. J. Bloom, T. L. Nicholson, J. R. Williams, S. L. Campbell, M. Bishof, X. Zhang, W. Zhang, S. L. Bromley, and J. Ye, *Nature* **506**, 71 (2014).
- [14] A. J. Daley, *Quantum Information Processing* **10**, 865 (2011).
- [15] N. Nonne, M. Molinear, S. Capponi, P. Lecheminant, and K. Totsuka, *Eur. Phys. Lett.* **102**, 37008 (2013).
- [16] H. Nonne, P. Lecheminant, S. Capponi, G. Roux, and E. Boulat, *Phys. Rev. B* **81**, 020408 (2010).
- [17] E. Szirmai, *Phys. Rev. B* **88**, 195432 (2013).
- [18] E. Szirmai, O. Legeza, and J. Sólyom, *Phys. Rev. B* **77**, 045106 (2008).
- [19] X.-W. Guan, M. T. Batchelor, and C. Lee, *Rev. Mod. Phys.* **85**, 1633 (2013).
- [20] G. Pagano and *et al*, *Nature Physics* **10**, 198 (2014).
- [21] M. A. Cazalilla, A. F. Ho, and M. Ueda, *New Journal of Physics* **11**, Artn 103033 Doi 10.1088/1367 (2009).
- [22] A. V. Gorshkov, M. Hermele, V. Gurarie, C. Xu, P. S. Julienne, J. Ye, P. Zoller, E. Demler, M. D. Lukin, and A. M. Rey, *Nature Physics* **6**, 289 (2010).
- [23] T. D. Lee, K. Huang, and C. N. Yang, *Phys. Rev.* **106**, 1135 (1957).
- [24] S.-K. Yip and T.-L. Ho, *Phys. Rev. A* **59**, 4653 (1999).
- [25] C. Chin, R. Grimm, P. Julienne, and E. Tiesinga, *Rev. Mod. Phys.* **82**, 1225 (2010).
- [26] C. J. Wu, J. P. Hu, and S. C. Zhang, *Phys. Rev. Lett.* **91**, 186402 (2003).
- [27] A. Modawi and A. J. Leggett, *Journal of Low Temperature Physics* **109**, 625 (1997).
- [28] C. Honerkamp and W. Hofstetter, *Phys. Rev. Lett.* **92**, 170403 (2004).
- [29] C. Honerkamp and W. Hofstetter, *Phys. Rev. B* **70**, 094521 (2004).
- [30] T. B. Ottenstein, T. Lompe, M. Kohnen, A. N. Wenz, and S. Jochim, *Phys. Rev. Lett.* **101**, 203202 (2008).
- [31] J. H. Huckans, J. R. Williams, E. L. Hazlett, R. W. Stites, and K. M. O'Hara, *Phys. Rev. Lett.* **102**, 165302 (2009).
- [32] M. M. Boyd, T. Zelevinsky, A. D. Ludlow, S. M. Foreman, S. Blatt, T. Ido, and J. Ye, *Science* **314**, 1430 (2006).
- [33] F. Gürsey and L. A. Radicati, *Phys. Rev. Lett.* **13**, 173 (1964).
- [34] L. He, M. Jin, and P. Zhuang, *Phys. Rev. A* **74**, 033604 (2006).
- [35] A. Rapp, G. Zaránd, C. Honerkamp, and W. Hofstetter, *Phys. Rev. Lett.* **98**, 160405 (2007).
- [36] T. Ozawa and G. Baym, *Phys. Rev. A* **82**, 063615 (2010).

- [37] M. Hermele, V. Gurarie, and A. M. Rey, Phys. Rev. Lett. **103**, 135301 (2009).
- [38] V. Kalmeyer and R. B. Laughlin, Phys. Rev. Lett. **59**, 2095 (1987).
- [39] X. G. Wen, F. Wilczek, and A. Zee, Phys. Rev. B **39**, 11413 (1989).
- [40] A. Kitaev, Annals of Physics (????).
- [41] N. Read and D. Newns, Advances in Physics **16**, 3273 (1983).
- [42] P. Coleman, Phys. Rev. B **28**, 5255 (1983).
- [43] N. Read and D. Newns, Advances in Physics **36**, 799 (1987).
- [44] I. Affleck and J. B. Marston, Phys. Rev. B **37**, 3774 (1988).
- [45] J. B. Marston and I. Affleck, Phys. Rev. B **39**, 11538 (1989).
- [46] N. Read and S. Sachdev, Nuclear Physics B **316**, 609 (1989).
- [47] D. P. Arovas, A. Karlhede, and D. Lilliehöök, Phys. Rev. B **59**, 13147 (1999).
- [48] Z. F. Ezawa, G. Tsitsishvili, and K. Hasebe, Phys. Rev. B **67**, 125314 (2003).
- [49] A. H. Castro Neto, F. Guinea, N. M. R. Peres, K. S. Novoselov, and A. K. Geim, Rev. Mod. Phys. **81**, 109 (2009).
- [50] M. O. Goerbig, Rev. Mod. Phys. **83**, 1193 (2011).
- [51] M. Kharitonov, Phys. Rev. Lett. **109**, 046803 (2012).
- [52] M. Kharitonov, Phys. Rev. B **86**, 075450 (2012).
- [53] M. O. Goerbig and N. Regnault, Phys. Rev. B **75**, 241405 (2007).
- [54] G. F. Gribakin and V. V. Flambaum, Phys. Rev. A **48**, 546 (1993).
- [55] M. Kitagawa, K. Enomoto, K. Kasa, Y. Takahashi, R. Ciurylo, P. Naidon, and P. S. Julienne, Phys. Rev. A **77**, 012719 (2008).
- [56] S. H. Autler and C. H. Townes, Phys. Rev. **100**, 703 (1955).
- [57] M. Kitagawa, K. Enomoto, K. Kasa, Y. Takahashi, R. Ciurylo, P. Naidon, and P. S. Julienne, Phys. Rev. A **77**, 012719 (2008).
- [58] Y. N. M. de Escobar, P. G. Mickelson, P. Pellegrini, S. B. Nagel, A. Traverso, M. Yan, R. Cote, and T. C. Killian, Phys. Rev. A **78**, 062708 (2008).
- [59] Y. Takasu, K. Maki, K. Komori, T. Takano, K. Honda, M. Kumakura, T. Yabuzaki, and Y. Takahashi, Phys. Rev. Lett. **91**, 040404 (2003).
- [60] T. Fukuhara, Y. Takasu, M. Kumakura, and Y. Takahashi, Phys. Rev. Lett. **98**, 030401 (2007).
- [61] T. Fukuhara, S. Sugawa, and Y. Takahashi, Phys. Rev. A **76**, 051604 (2007).
- [62] T. Fukuhara, S. Sugawa, Y. Takasu, and Y. Takahashi, Phys. Rev. A **79**, 021601 (2009).
- [63] S. Taie, Y. Takasu, S. Sugawa, R. Yamazaki, T. Tsujimoto, R. Murakami, and Y. Takahashi, Phys. Rev. Lett. **105**, 190401 (2010).
- [64] S. Sugawa, R. Yamazaki, S. Taie, and Y. Takahashi, Phys. Rev. A **84**, 011610 (2011).
- [65] S. Dorscher, A. Thobe, B. Hundt, A. Kochanke, R. L. Targat, P. Windpassinger, C. Becker, and K. Sengstock, Review of Scientific Instruments **84**, 043109 (2013).
- [66] A. H. Hansen, A. Khramov, W. H. Dowd, A. O. Jamison, V. V. Ivanov, and S. Gupta, Phys. Rev. A **84**, 011606

(2011).

- [67] H. Hara, Y. Takasu, Y. Yamaoka, J. M. Doyle, and Y. Takahashi, Phys. Rev. Lett. **106**, 205304 (2011).
- [68] S. Kraft, F. Vogt, O. Appel, F. Riehle, and U. Sterr, Phys. Rev. Lett. **103**, 130401 (2009).
- [69] P. Halder, C.-Y. Yang, and A. Hemmerich, Phys. Rev. A **85**, 031603 (2012).
- [70] T. Ido, Y. Isoya, and H. Katori, Phys. Rev. A **61**, 061403 (2000).
- [71] G. Ferrari, R. E. Drullinger, N. Poli, F. Sorrentino, and G. M. Tino, Phys. Rev. A **73**, 023408 (2006).
- [72] S. Stellmer, M. K. Tey, B. Huang, R. Grimm, and F. Schreck, Phys. Rev. Lett. **103**, 200401 (2009).
- [73] Y. N. M. de Escobar, P. G. Mickelson, M. Yan, B. J. DeSalvo, S. B. Nagel, and T. C. Killian, Phys. Rev. Lett. **103**, 200402 (2009).
- [74] M. K. Tey, S. Stellmer, R. Grimm, and F. Schreck, Phys. Rev. A **82**, 011608 (2010).
- [75] B. J. DeSalvo, M. Yan, P. G. Mickelson, Y. N. M. de Escobar, and T. C. Killian, Phys. Rev. Lett. **105**, 030402 (2010).
- [76] S. Stellmer, M. K. Tey, R. Grimm, and F. Schreck, Phys. Rev. A **82**, 041602 (2010).
- [77] S. Stellmer, R. Grimm, and F. Schreck, Phys. Rev. A **87**, 013611 (2013).
- [78] P. G. Mickelson, Y. N. M. de Escobar, M. Yan, B. J. DeSalvo, and T. C. Killian, Phys. Rev. A **81**, 051601 (2010).
- [79] S. Stellmer, B. Pasquiou, R. Grimm, and F. Schreck, Phys. Rev. Lett. **110**, 263003 (2013).
- [80] R. Ciurylo, E. Tiesinga, and P. S. Julienne, Phys. Rev. A **71**, 030701 (2005).
- [81] K. Enomoto, K. Kasa, M. Kitagawa, and Y. Takahashi, Phys. Rev. Lett. **101**, 203201 (2008).
- [82] R. Yamazaki, S. Taie, S. Sugawa, and Y. Takahashi, Phys. Rev. Lett. **105**, 050405 (2010).
- [83] S. Blatt, T. L. Nicholson, B. J. Bloom, J. R. Williams, J. W. Thomsen, P. S. Julienne, and J. Ye, Phys. Rev. Lett. **107**, 073202 (2011).
- [84] M. Yan, B. J. DeSalvo, B. Ramachandhran, H. Pu, and T. C. Killian, Phys. Rev. Lett. **110**, 123201 (2013).
- [85] I. H. Deutsch and P. S. Jessen, Phys. Rev. A **57**, 1972 (1998).
- [86] S. Stellmer, R. Grimm, and F. Schreck, Phys. Rev. A **84**, 043611 (2011).
- [87] M. M. Boyd, T. Zelevinsky, A. D. Ludlow, S. Blatt, T. Zanon-Willette, S. M. Foreman, and J. Ye, Phys. Rev. A **76**, 022510 (2007).
- [88] J. Ye, H. J. Kimble, and H. Katori, Science **320**, 1734 (2008).
- [89] M. Greiner and S. Folling, Nature **453**, 736 (2008).
- [90] M. A. Cazalilla, R. Citro, T. Giamarchi, E. Orignac, and M. Rigol, Reviews of Modern Physics **83**, 1405 Doi 10.1103/RevModPhys.83.1405 (2011).
- [91] T. Stöferle, H. Moritz, C. Schori, M. Köhl, and T. Esslinger, Phys. Rev. Lett. **92**, 130403 (2004).
- [92] A. Iucci, M. A. Cazalilla, A. F. Ho, and T. Giamarchi, Phys. Rev. A **73**, 041608 (2006).
- [93] C. Kollath, A. Iucci, I. P. McCulloch, and T. Giamarchi, Phys. Rev. A **74**, 041604 (2006).
- [94] A. Tokuno and T. Giamarchi, Phys. Rev. A **85**, 061603 (2012).
- [95] S. Taie, R. Yamazaki, S. Sugawa, and Y. Takahashi, Nature Physics **8**, 825 (2012).
- [96] K. R. A. Hazzard, V. Gurarie, M. Hermele, and A. M. Rey, Phys. Rev. A **85**, 041604 (2012).

- [97] L. D. Landau, Sov. Phys. JETP **3**, 920 (1975).
- [98] G. Baym and C. Pethick, *Landau Fermi-Liquid Theory* (Wiley, 1991).
- [99] G. Y. Chitov and D. Sénéchal, Phys. Rev. B **52**, 13487 (1995).
- [100] S.-K. Yip and J.-S. Huang, B.-L. Kao, preprint [arXiv:1312.6765](https://arxiv.org/abs/1312.6765) (2013).
- [101] D. Belitz and T. R. Kirkpatrick, Phys. Rev. Lett. **89**, 247202 (2002).
- [102] R. A. Duine and A. H. MacDonald, Phys. Rev. Lett. **95**, 230403 (2005).
- [103] M. A. Cazalilla, unpublished (????).
- [104] P.-N. Ma, S. Pilati, M. Troyer, and X. Dai, Nat. Phys. **8**, 601 (2008).
- [105] A. Rapp and A. Rosch, Phys. Rev. A **83**, 053605 (2011).
- [106] H. Katsura and A. Tanaka, Phys. Rev. A **87**, 013617 (2013).
- [107] S. Nascimbene, N. Navon, K. J. Jiang, F. Chevy, and C. Salomon, Nature **463**, 1057 (2010).
- [108] S. Nascimbene, N. Navon, F. Chev, and C. Salomon, New J. of Phys. **12**, 103026 (2010).
- [109] J. R. Schrieffer, *Theory Of Superconductivity* (Westview Press, 1971).
- [110] W. Kohn and J. Luttinger, Phys. Rev. Lett. **109**, 230801 (2012).
- [111] R. W. Cherng, G. Refael, and E. Demler, Phys. Rev. Lett. **99**, 130406 (2007).
- [112] S.-K. Yip, Phys. Rev. A **83**, 063607 (2011).
- [113] D. C. Youla, Can. J. of Math. **13**, 694 (1961).
- [114] S. Lang, *Algebra, Revised 3rd edition (pag.586 and ff.)* (Springer Verlag, 2000).
- [115] P. Nozères and S. Schmitt-Rink, J. of Low Temp. Phys. **59**, 331 (1984).
- [116] L. D. Landau and E. M. Lifshitz, *Statistical Mechanics, 3rd edition* (Pergamon Press, 1957).
- [117] G. Klingschat and C. Honerkamp, Phys. Rev. B **82**, 094521 (2010).
- [118] L. Bonnes, K. R. A. Hazzard, S. R. Manmana, A. M. Rey, and S. Wessel, Phys. Rev. Lett. **109**, 205305 (2012).
- [119] L. Messio and F. d. r. Mila, Phys. Rev. Lett. **109**, 205306 (2012).
- [120] K. Lee, Physics Letters A **187**, 112 (1994).
- [121] S. R. Manmana, K. R. A. Hazzard, G. Chen, A. E. Feiguin, and A. M. Rey, Phys. Rev. A **84**, 043601 (2011).
- [122] R. Assaraf, P. Azaria, M. Caffarel, and P. Lecheminant, Phys. Rev. B **60**, 2299 (1999).
- [123] B. Sutherland, Phys. Rev. B **12**, 3795 (1975).
- [124] D. A. Ivanov, P. A. Lee, and X.-G. Wen, Phys. Rev. Lett. **84**, 3958 (2000).
- [125] M. Hermele and V. Gurarie, Phys. Rev. B **84**, 174441 (2011).
- [126] T. A. Toth, A. M. Lauchli, F. Mila, and K. Penc, Phys. Rev. Lett. **105**, 265301 (2010).
- [127] P. Corboz, A. M. Lauchli, K. Penc, M. Troyer, and F. Mila, Phys. Rev. Lett. **107**, 215301 (2011).
- [128] F. F. Assaad, Phys. Rev. B **71**, 075103 (2005).
- [129] D. S. Rokhsar, Phys. Rev. B **42**, 2526 (1990).
- [130] V. Kalmeyer and R. B. Laughlin, Phys. Rev. B **39**, 11879 (1989).
- [131] A. L²lauchli, F. Mila, and K. Penc, Phys. Rev. Lett. **97**, 087205 (2006).
- [132] H. H. Zhao, C. Xu, Q. N. Chen, Z. C. Wei, M. P. Qin, G. M. Zhang, and T. Xiang, Phys. Rev. B **85**, 134416 (2012).

- [133] Y.-W. Lee and M.-F. Yang, Phys. Rev. B **85**, 100402 (2012).
- [134] P. Corboz, M. Lajkó, K. Penc, F. Mila, and A. M. Läuchli, Phys. Rev. B **87**, 195113 (2013).
- [135] G. Szirmai, E. Szirmai, A. Zamora, and M. Lewenstein, Phys. Rev. A **84**, 011611 (2011).
- [136] P. Corboz, M. Lajkó, A. M. Läuchli, K. Penc, and F. Mila, Phys. Rev. X **2**, 041013 (2012).
- [137] A. J. Daley, M. M. Boyd, J. Ye, and P. Zoller, Phys. Rev. Lett. **101**, 170504 (2008).
- [138] A. D. Ludlow, N. D. Lemke, J. A. Sherman, C. W. Oates, G. Qumner, J. von Stecher, and A. M. Rey, Phys. Rev. A **84**, 052724 (2011).
- [139] M. Bishof, Y. Lin, M. D. Swallows, A. V. Gorshkov, J. Ye, and A. M. Rey, Physical Review Letters **106**, 250801 (2011).
- [140] M. Foss-Feig, M. Hermele, V. Gurarie, and A. M. Rey, Physical Review A **82**, 053624 (2010).
- [141] M. Foss-Feig, M. Hermele, and A. M. Rey, Physical Review A **81**, 051603 (2010).
- [142] Y. Tokura, *Colossal Magnetoresistive Oxides* (Taylor and Francis, 2000).
- [143] P. Coleman, *Heavy Fermions: Electrons at the Edge of Magnetism* (John Wiley and Sons, Ltd, 2007).
- [144] Y. Tokura and N. Nagaosa, Science **288**, 462 (2000).
- [145] M. Freedman, C. Nayak, K. Shtengel, K. Walker, and Z. Wang, Annals of Physics **310**, 428 (2004).
- [146] G. Moore and N. Read, Nuclear Physics B **360**, 362 (1991).
- [147] R. L. Willett, L. N. Pfeiffer, and K. W. West, Phys. Rev. B **82**, 205301 (2010).
- [148] J. Alicea, Y. Oreg, G. Refael, F. von Oppen, and M. P. A. Fisher, Nat Phys **7**, 412 (2011).
- [149] C. Nayak, S. H. Simon, A. Stern, M. Freedman, and S. D. Sarma, Rev. Mod. Phys. **80**, 1083 (2008).
- [150] J. Dalibard, F. Gerbier, G. Juzelanas, and P. Ahberg, Rev. Mod. Phys. **83**, 1523 (2010).
- [151] I. B. Spielman, Nature **472**, 301 (2011).
- [152] Y. J. Lin, K. Jimenez-Garcia, and I. B. Spielman, Nature **471**, 83 (2011).
- [153] L. W. Cheuk, A. T. Sommer, Z. Hadzibabic, T. Yefsah, W. S. Bakr, and M. W. Zwierlein, Phys. Rev. Lett. **109**, 095302 (2012).
- [154] C. J. Kennedy, G. A. Siviloglou, H. Miyake, W. C. Burton, and W. Ketterle, Phys. Rev. Lett. **111**, 225301 (2013).
- [155] H. Miyake, G. A. Siviloglou, C. J. Kennedy, W. C. Burton, and W. Ketterle, Phys. Rev. Lett. **111**, 185302 (2013).
- [156] M. Aidelsburger, M. Atala, M. Lohse, J. T. Barreiro, B. Paredes, and I. Bloch, Phys. Rev. Lett. **111**, 185301 (2013).
- [157] F. Gerbier and J. Dalibard, New Journal of Physics **12**, 033007 (2010).
- [158] N. R. Cooper, Phys. Rev. Lett. **106**, 175301 (2011).
- [159] N. R. Cooper and J. Dalibard, Phys. Rev. Lett. **110**, 185301 (2013).
- [160] D. Banerjee, M. Bogli, M. Dalmonte, E. Rico, P. Stebler, U. J. Wiese, and P. Zoller, Phys. Rev. Lett. **110**, 125303 (2013).
- [161] N. Goldman, F. Gerbier, and M. Lewenstein, Journal of Physics B: Atomic, Molecular and Optical Physics **46**, 134010 (2013).

- [162] M. Swallows, M. Martin, M. Bishof, C. Benko, Y. Lin, S. Blatt, A. M. Rey, and Y. J., Proceedings Joint IFCS/EFTF (2011).
- [163] A. M. Rey, A. V. Gorshkov, and C. Rubbo, Phys. Rev. Lett. **103**, 260402 (2009).
- [164] K. Gibble, Physical Review Letters **103**, 113202 (2009).
- [165] N. D. Lemke, J. VonStecher, J. A. Sherman, A. M. Rey, C. W. Oates, and A. D. Ludlow, Physical Review Letters **107**, 103902 (2011).
- [166] M. D. Swallows, M. Bishof, Y. G. Lin, S. Blatt, M. J. Martin, A. M. Rey, and J. Ye, Science **331**, 1043 (2011).
- [167] M. Foss-Feig, A. J. Daley, J. K. Thompson, and A. M. Rey, Phys. Rev. Lett. **109**, 230501 (2012).
- [168] M. J. Martin, M. Bishof, M. D. Swallows, X. Zhang, C. Benko, J. von Stecher, A. V. Gorshkov, A. M. Rey, and J. Ye, Science **341**, 632 (2013).
- [169] A. Rey, A. Gorshkov, C. Kraus, M. Martin, M. Bishof, M. Swallows, X. Zhang, C. Benko, J. Ye, N. Lemke, et al., Annals of Physics **340**, 311 (2014).
- [170] D. Meiser, J. Ye, D. R. Carlson, and M. J. Holland, Phys. Rev. Lett. **102**, 163601 (2009).
- [171] B. Olmos, D. Yu, Y. Singh, F. Schreck, K. Bongs, and I. Lesanovsky, Phys. Rev. Lett. **110**, 143602 (2013).
- [172] J. G. Bohnet, Z. L. Chen, J. M. Weiner, D. Meiser, M. J. Holland, and J. K. Thompson, Nature **484**, 78 (2012).
- [173] H. Watanabe and H. Murayama, Phys. Rev. Lett. **108**, 251602 (2012).
- [174] An exception is the Kondo problem discussed in Refs. [41–43], for which N corresponds to the number of possible degenerate magnetic configurations of the impurity atom.
- [175] Henceforth, we adopt the Einstein convention, which implies that summation must be implicitly understood over repeated Greek indices unless otherwise stated.